Deliverable D13.7: Final report on combined measurement/model activities

Coordinating author: Angela Benedetti (ECMWF)
Contributor lists (in alphabetical order for each institute):
Sara Basart, Enza Di Tomaso, Jeronimo Escribano, Oriol Jorba, Francesca Macchia, Carlos Perez Garcia-Pando (BSC);
Qiaoyun Hu, Philippe Goloub (Universite de Lille)
Claudia Urbanneck, Holger Baars, Albert Ansmann, Ulla Wandinger (TROPOS);
Lucia Mona, Nikolao Papagiannopoulos, Giuseppe D'Amico (CNR-IMAA);
Enric Terradellas, Gerardo García-Castrillo, Emilio Cuevas (AEMET, Spain);
Lucas Alados-Arboledas, Alberto Cazorla (Universidad de Granada, Spain);
Andrés Alastuey, Marco Pandolfi (CSIC-IDAEA, Spain)
Melanie Ades, Angela Benedetti, Luke Jones, Zak Kipling, Julie Letertre-Danczak, (ECMWF)
Hendrik Elbern, Anne Caroline Lange (RIUUK)

Work package no	**WP13**		
Deliverable no.	**D13.7**		
Lead beneficiary			
Deliverable type	☑	R (Document, report)	
	☐	DEC (Websites, patent fillings, videos, etc.)	
	☐	OTHER: please specify **……………………………………….**	
Dissemination level	☑	PU (public)	
	☐	CO (confidential, only for members of the Consortium, incl Commission)	
Estimated delivery date	**Month 46**		
Actual delivery date	***Month 48***		
Version			
Comments	*Delayed due to administrative issues*		

D13.7: FINAL REPORT ON COMBINED MEASUREMENT/MODEL ACTIVITIES

1 INTRODUCTION

Aerosol observations are key to the advancement of our understanding of the role of aerosols in many fundamental areas such as climate change, weather impacts and air quality. Without high quality observations, models are not able to produce meaningful predictions as they cannot be bench-marked or verified. In recent years, much effort has been put in coordinating international activities to create and harmonize observing networks from existing regional or national sites. Pivotal in this development has been the funding of the two phases of the European project Aerosols, Clouds, and Trace gases Research InfraStructure (ACTRIS) which has brought together many data providers and offered transnational access to the observing facilities while also fostering technological developments in instrumentation and retrieval techniques. ACTRIS is also the European component of the World Meteorological Organization (WMO) Global Atmosphere Watch (GAW) and as such its data centre hosts both Europen and global data. In its second phase, started in 2015, ACTRIS has also fostered collaboration between data providers and model developers by funding a Joint Research Activity (JRA) which has been undertaken in WP13. Several European research and operational institutes with interest in aerosol science have been involved (see list of contributors). This report showcases some of the results obtained from this collaboration. As such, the results presented are diverse and range from the assimilation of dust and volcanic ash profiles to improve model prediction to pre-operational verification using previously untapped data sources such as surface-based light scattering and absorption observations. Companion reports, already delivered, showed the value of the measurements in the reduction in global model errors (D13.5) and the use of the measurement for a detailed analysis of the aerosol trends (D13.6). These results from JRA3 show how ACTRIS observations are powerful means to test, improve and evaluate models and to understand changes in the aerosol distribution.

2 VERIFICATION ACTIVITIES

2.1 MODEL EVALUATION AND ONLINE VERIFICATION OF DUST FORECASTS

One of the most important activities of the World Meteorological Organization's Sand and Dust Storm Warning Advisory and Assessment System - Northern Africa-Middle East-Europe Regional Center (WMO SDS-WAS NAMEE RC, http://sds-was.aemet.es) is the dust model verification and evaluation, which is deemed an indispensable service to the users and an invaluable tool to assess model skills. Currently, the Center collects daily dust forecasts from twelve models run by different partners (BSC, ECMWF, NASA, NCEP, SEEVCCC, EMA, CNR-ISAC, NOA, FMI, TNO and UK Met Office). Multi-model ensembles have also been set-up to provide added-value aerosol products to the users. The current routine evaluation of dust predictions is focused on total-column dust optical depth (DOD) and uses remote-sensing retrievals from sun-photometric (AERONET and particularly, AERONET-Europe which is under the umbrella of ACTRIS) and satellite (MODIS) measurements. However, the Regional Center started working in the establishment of a near-real-time (NRT) model monitoring/evaluation dust profile system.

Ground- and satellite-borne lidar and last generation of ceilometers are the only tools capable of inquiring about the vertical profiles of aerosol-related variables. Therefore, information provided by them may potentially be used to evaluate the vertical component of the dust fields. On the one hand, research activities are indispensable, e.g., to improve our understanding of interactions of aerosols and clouds, and to develop advanced remote sensing techniques (fundamentally based on lidars systems) for the assessment of optical and microphysical aerosol properties. As a consequence of the complexity of the lidar systems, they are quite expensive; thus their number is limited, and many of them are operated by research institutes only

occasionally or during dedicated field campaigns. On the other hand, infrastructures must be implemented to monitor aerosols also to validate and improve aerosol and pollution forecasting with high spatial and temporal coverage as well as, with low-cost and low-maintenance instruments. Significant progress in range-resolved aerosol characterization is accomplished using lidar technology as they can provide quantitative range-resolved aerosol parameters. However, currently, costs for investment and maintenance of advanced near-real-time lidar systems are prohibitive for establishing dense networks. Despite their differences from more advanced and more powerful lidars, low construction and operation cost of ceilometer, originally designed for cloud base height monitoring, have fostered their use for the quantitative study of aerosol properties (i.e. Wiegner et al., 2014; Madonna et al. 2016). A large number of ceilometers available worldwide represent a potential observational dataset for operational dust model evaluation purposes. Additionally, ceilometer measurements can benefit from ACTRIS/EARLINET lidar primarily for calibration (Weigner et al., 2014).

E-PROFILE (http://eumetnet.eu/glossary/e-profile/) coordinates the measurements of vertical profiles from a network of locations across Europe and provides the data to the end users in near-real-time. This network is part of the EUMETNET Composite Observing System, EUCOS, managing the European networks of radar wind profilers (RWP) and automatic lidars and ceilometers (ALC) for the monitoring of vertical profiles of wind and aerosols including volcanic ash. The main goal of E-profile is to improve the overall usability of wind and aerosol profiler data for operational meteorology and to provide support and expertise to both profiler operators and end users. To make available this new observation capacity, E-profile is developing a framework to produce and exchange profiles of attenuated backscatter profiles (https://ceilometer.e-profile.eu/).

Currently, a lidar (monoaxial Cimel Micro-Pulsed Lidar, CAML CE-370, starting in September 2015) located in M'Bour-Dakar (Senegal, U. Lille, part of ACTRIS-France) and three ceilometers in Santa Cruz de Tenerife (Canary Islands, Spain, CIAI-AEMET, starting in July 2015), Granada (Spain, University of Granada, starting in January 2016) and Montsec (Barcelona, Spain, CSIC-IDAEA, starting in January 2016) provide NRT extinction profiles of aerosols to the WMO SDS-WAS NAMME RC (see Figure 1). The lidar in Dakar (Mortier et al., 2016) was installed in the context of the African Monsoon Multidisciplinary Analyses campaign in 2005 and, the three ceilometers are part of the Iberian Ceilometer Network (ICENET, Cazorla et al. 2017) and they are also considered in E-profile.

Figure 1: Location of those sites that are providing NRT extinction profiles to the SDS-WAS NAMEE RC. Lidars are shown in black and ceilometers in red.

Otherwise, the exchange of forecast model products (and consequently, data harmonisation) is recognised as a core part of the WMO SDS-WAS NAMEE RC and as a basis for the model inter-comparison and evaluation. Within this objective, a protocol has been defined for model data exchange. The format for data exchange is NetCDF, with one file per model run and includes the resulting interpolated model outputs from a list of stations (which includes all the ACTRIS/EARLINET sites and additional key locations). The action will consider forecasts with lead times up to 72 h, based on 00 UTC or 12 UTC runs on 3-hourly basis. The variables to be provided are: dust concentration, dust extinction (at 550 nm) and the corresponding height of each model layer. Currently, the BSC-DREAM8b and the NMMB/BSC-Dust (the mineral dust module of the NMMB-MONARCH model) models provide operational dust forecast profiles.
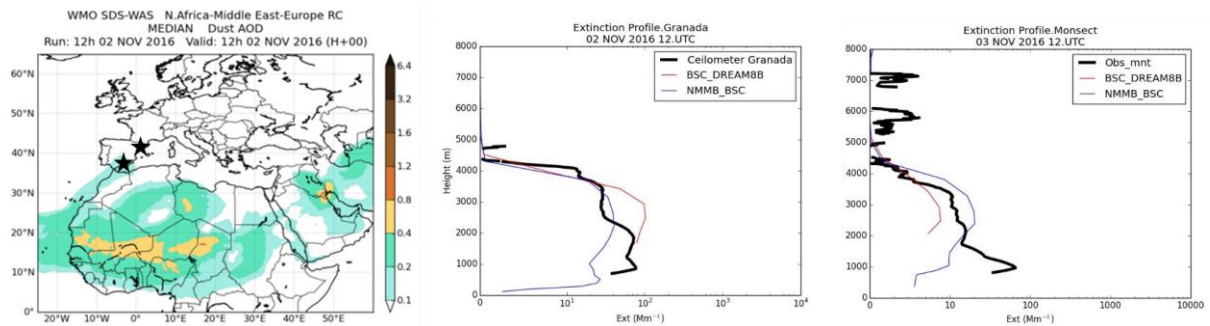

Figure 2. Example of compared aerosol profile from the SDS-WAS NAMEE RC website for 2 November 2016 at 12UTC. Left: SDS-WAS Multi-model Dust AOD product. Stars indicated the locations of the profiles depicted in central and right panels. Central: Compared aerosol profiles in Granada, Spain. Right: Compared aerosol profiles in Santa Cruz de Tenerife, Canary Islands. BSC-DREAM8b (red) and NMMB/BSC-Dust (blue) dust forecasts and lidar (black) operated by the University of Lille. BSC-DREAM8b (red) and NMMB/BSC-Dust (blue) dust forecasts and ceilometer (black) operated by the Izana Atmospheric Reseach Center - AEMET.
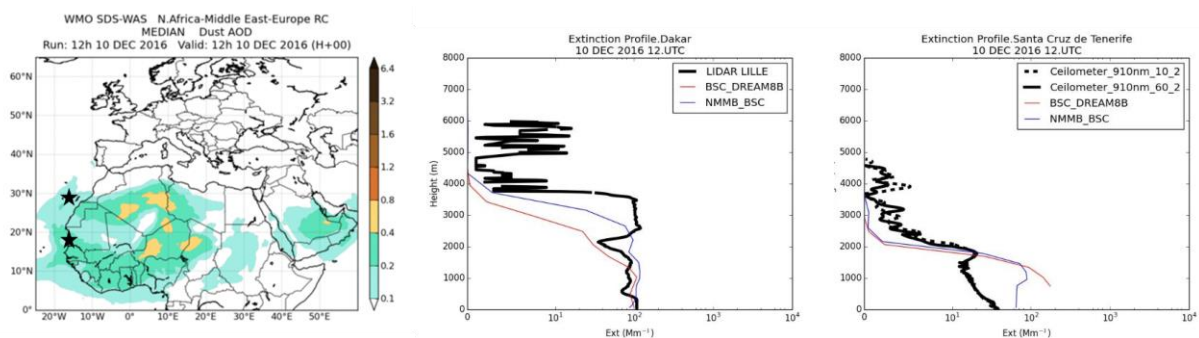

Figure .3. Example of compared aerosol profile from the SDS-WAS NAMEE RC website for 10 December 2016 at 12UTC. Left: SDS-WAS Multi-model Dust AOD product. Stars indicated the locations of the profiles depicted in central and right panels. Central: Compared aerosol profiles in Dakar, Senegal. BSC-DREAM8b (red) and NMMB/BSC-Dust (blue) dust forecasts and lidar (black) operated by the University of Lille. Right: Compared aerosol profiles in Santa Cruz de Tenerife, Canary Islands. BSC-DREAM8b (red) and NMMB/BSC-Dust (blue) dust forecasts and ceilometer (black) operated by the Izana Atmospheric Reseach Center - AEMET.

All the available data is routinely used to generate qualitatively comparison plots for each specific location. This was the first step to check the consistency of the received data and the agreement between observations and dust forecasts during intense dust events on the location of the dust layer as on 2nd November 2016 (see Figure 2) and 10th December 2016 (see Figure 3). All the numerical data is available through the SDS-

WAS NAMEE RC website (http://sds-was.aemet.es/projects-research/evaluation-of-model-derived-dust-vertical-profiles).

Next step included the development of a quantitative evaluation methodology which includes considerations for the selection of a suitable data set and appropriate metrics for the exploration of the results. Many of dust model evaluation analysis have focused on a limited number of case studies (e.g., Pérez et al., 2006; Heinold et al., 2009; Granados-Muñoz et al., 2016). In other studies, long-term observations of aerosol optical properties have been compared with modelled dust optical profiles. For example, Gobbi et al. (2013) compared the lidar dust extinction profiles with those modelled by BSC-DREAM8b over Rome, Italy during the 2001–2004 period. Similarly, Mona et al. (2014) have presented a systematic examination of BSC-DREAM8b modelled dust distribution over Potenza, Italy, for the 2000–2012 period, using lidar-derived backscatter and extinction profiles.

Moreover, Mona et al. (2014) found that the dust layer centre of mass (CoM) is likely the most suitable geometrical parameter for evaluating the capability of the dust model to reproduce the vertical dust layering. Recently, Binietoglou et al. (2015) introduced a methodology for the examination of dust model data using volume concentration profiles retrieved using the synergy of lidar and sun photometer. The approach was demonstrated for four regional dust transport models participating in the SDS-WAS Regional Node (BSC-DREAM8b v2, NMMB/BSC-DUST, DREAMABOL, DREAM8-NMME-MACC) using dust observations performed at 10 ACTRIS/EARLINET stations for the period between 2011-2013.
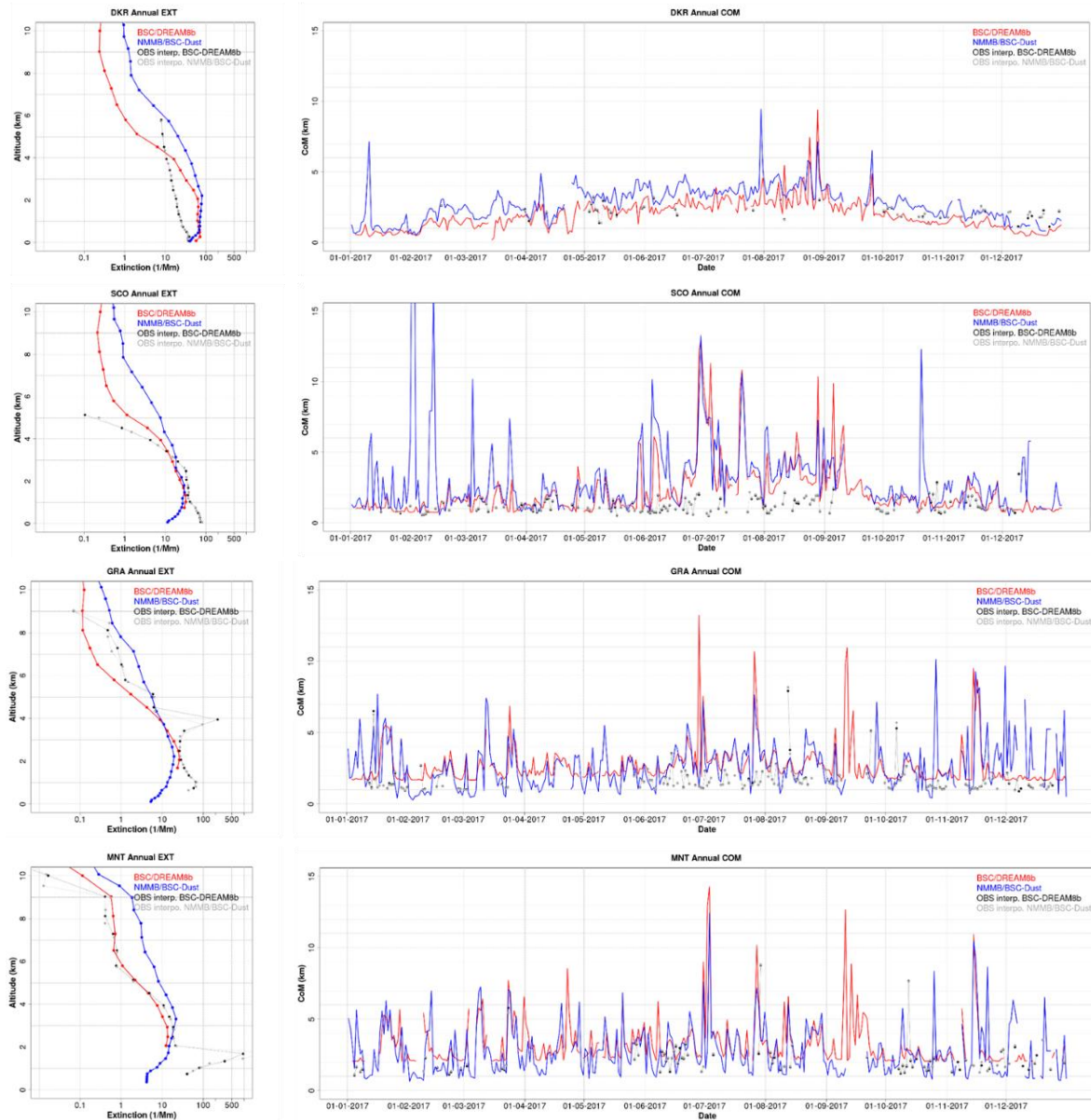
Figure 4: Compared aerosol profiles for the year 2017. The comparison includes BSC-DREAM8b (red) and NMMB/BSC-Dust (blue) dust forecasts and lidar/celilometers (black) at Dakar, Santa Cruz de Tenerife, Granada and Montsec. Rigth: Annual extinction profile. Left: Time series of the Center of Mass (COM). Observations are interpolated to the original model vertical layers. The BSC-DREAM uses ETA-levels and the NMMB/BSC-Dust σ-levels.

Following these preliminary experiences, the extinction profiles obtained in the four locations considered in this exercise during the year 2017 were interpolated to the original model vertical layers of the two models participating, i.e. BSC-DREAM8b and NMMB/BSC-Dust for comparison (see Figure 4). In general, the comparison shows how the models can reproduce the annual vertical aerosol distribution. More specifically:

- Vertical interpolation is sensible to the original model and observations vertical resolution. This causes differences in the observed CoM of up to 500m in some days in Montsec and Granada depending on the model coordinates considered.
- The high stratification of the atmosphere in the region of the North Atlantic reduce the laser signal. In Santa Cruz de Tenerife, the valid vertical range of the signal is limited to $< 4km$.
- The contribution aerosols particularly at lower levels within the PBL (see the annual average extinction profile of Montsec and Granada at $< 2km$) and/or maritime boundary layer (see the annual average extinction profile of Santa Cruz de Tenerife at $< 1km$) causes the overestimation of the CoM predicted by the models (see the time series in Figure 4).
- In Dakar, there is a weak agreement between observation and models in the annual average comparison despite that the models can simulate the seasonal behaviour of CoM with maximum altitude in summer (up to 4km) and minimum in winter (up to 1km).
- To define the top and the base of the dust layer in the case of the observations is complex when there are multiple dust layers or when the layer is inside the PBL giving some large discrepancies between models and observations.

To conclude, some recommendations for the implementation of a quantitative NRT verification system based on the calculation of the CoM, top and base of the dust layer observed by the lidar/ceilometers and predicted by the models:

- Vertical interpolation is sensible to the original model and observations vertical resolution. Therefore, the most standard product should be produced on standard pressure levels.
- The calculations of the CoM, top and base must include characteristics of each site, i.e. a valid range for the calculations that will take into account the instrument (intensity of the signal) and the aerosol characterization (top of the PBL and/or the maritime boundary layer).

2.2 MODEL EVALUATION AND ONLINE VERIFICATION OF AEROSOL SCATTERING AND ABSORPTION COEFFICIENTS

Under the projects GEMS (Hollingworth et al 2008) and MACC (Peuch and Engelen, 2012), ECMWF has developed a fully-integrated Earth-system model for atmospheric composition (the Integrated Forecast System, IFS, in composition configuration), now operationalized by the Copernicus Atmosphere Monitoring Service (CAMS). Aerosol forecasts are provided daily, up to 5 days from the global model. The forecasts are initialized with a 4D-Var analysis which uses aerosol optical depth (AOD) retrievals from the Moderate Resolution Imaging Spectroradiometer (MODIS) on NASA's Terra and Aqua satellites (Benedetti et al 2009). The EUMETSAT Polar Multi-sensor Aerosol properties (PMAp) AODs are also assimilated operationally. The resolution of the global forecasts is 40 km. To allow for regional pollution forecasts, global analyses are provided as boundary conditions for the regional air quality models that are part of CAMS and provide multi-model forecasts of pollution over Europe (domain: 20°W/30°N/45°E/70°N, see https://atmosphere.copernicus.eu/air-quality for further information) at higher resolution.

The multi-model ensemble model (so called CAMS regional Ensemble) is based on seven state-of-the-art numerical air quality models developed in Europe. They are combined via an ensemble approach, consisting in calculating the median value of the individual outputs. Currently, the models involved in Ensemble production are: CHIMERE from INERIS (France), EMEP from MET Norway (Norway), EURAD-IM from

ACTRIS (www.actris.eu) is supported by the European Commission under the Horizon 2020 – Research and Innovation Framework Programme, H2020-INFRAIA-2014-2015, Grant Agreement number: 654109

Page **7 / 30**

University of Cologne (Germany), LOTOS-EUROS from KNMI and TNO (The Netherlands), MATCH from SMHI (Sweden), MOCAGE from MeteoFrance (France) and SILAM from FMI (Finland).

The quality of the regional Ensemble depends, among other factors, on the quality of the boundary conditions that are provided by the global model. To understand the quality of the global model, the aerosols forecasts are verified routinely using ground-based AODs from AERONET stations (Holben et 2001). While this has proven a very powerful set of observations to evaluate the quality of the model, it was felt that more diverse observations were needed to identify model biases, particularly at the surface. AOD is a column-integrated quantity and hence does not reveal potential model problems related to the vertical distribution of the aerosols. However, the most important level for applications such as regional pollution forecasts is the surface, where human activities take place. It could happen that the total AOD in the model agrees perfectly with the observations, but the surface values of aerosol concentrations are wrong.

The need for a more thorough verification of the model performance at the surface has been a focus of WP13 verification activities at ECMWF. Aerosol absorption and scattering properties measured by the surface-based network of nephelometers and collected at NILU have been used for this purpose. In order to make use of these observations, the model fields of scattering and absorption coefficients were extracted at different wavelengths and for different values of ambient humidity (0% and 50% percent) at the model surface. The dependence on humidity for the two parameters is well established. Measurements are provided at an indicative ambient relative humidity of 40%,. hence the values of the scattering and absorption coefficients at 0 and 50% can be considered as a lower and upper boundary.

For the initial tests, one year of continuous comparisons from November 2016 to November 2017 was performed at all stations delivering in near-real-time (NRT). As an example, Figure 5 presents the comparison between the observations of the nephelometer located at Cabauw (51.98N, 4.93E, top panel), at Ispra (45.80N,8.63E, middle panel) and Puy de Dome (45.77N, 2.95E, bottom panel) and model output at two values of relative humidity (0 and 50%) at 550nm. The agreement between the observation and the model is good for the two sites of Cabauw and Ispra, despite the fact that the model has difficulties to reproduce some extreme values recorded between January and March. For the site of Puy de Dome the altitude of the site is an issue as the value at surface given by the model do not take account of topography with enough detail at the model resolution of ~80x80 km^2. For mountain sites, a meaningful comparison would entail rescaling the model output at the correct surface altitude using a high-resolution topography.
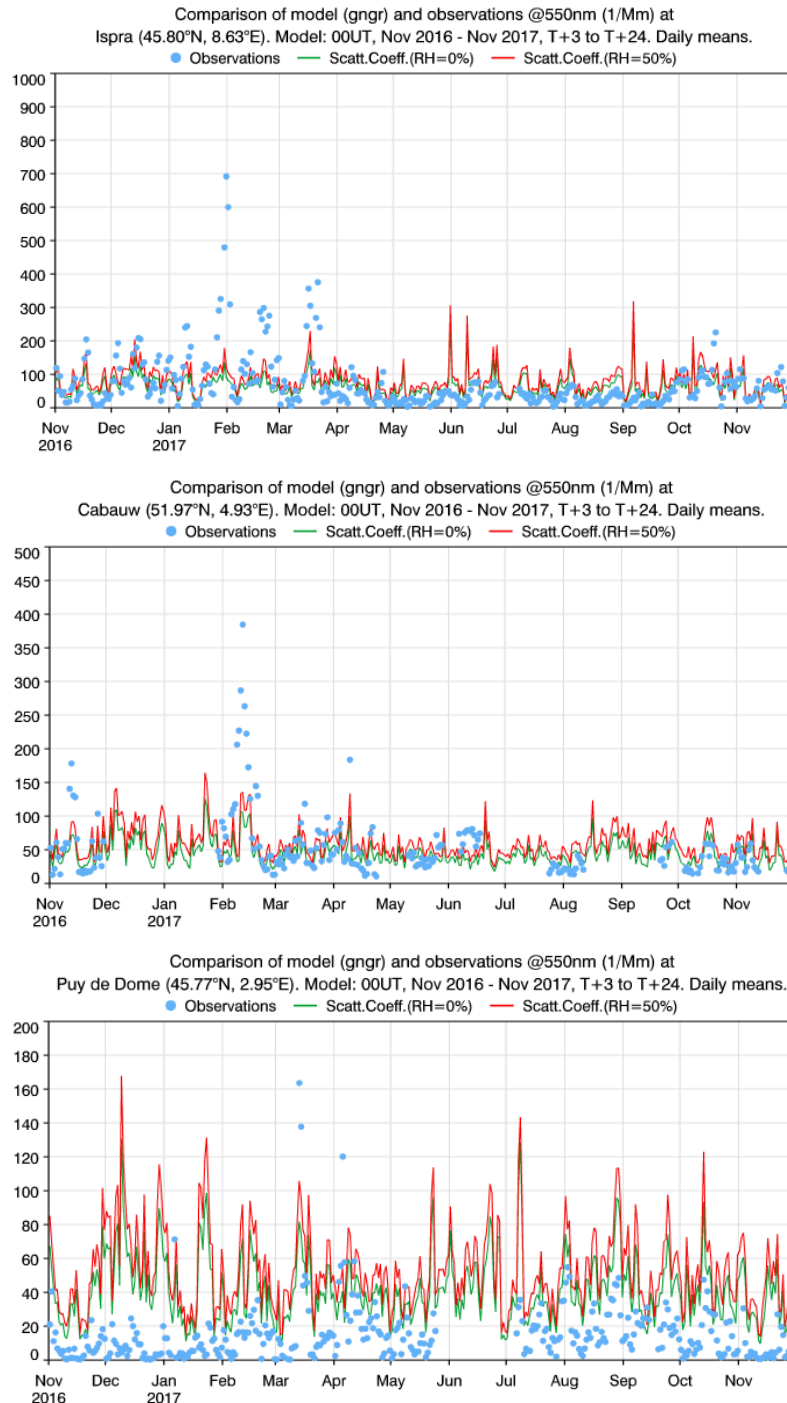
Figure 5. Comparison on scattering coefficient between daily mean observations from nephelometer (blue) with the model computed for 0% humidity (green) and 50% (red) during the period 11/2016 – 11/2017 for the sites of Cabauw, Ispra and Puy de Dome.

Since the results of this model-observation continuous comparison can be useful both for ECMWF as well as for the data providers, it has been decided to extend the verification to near-real time and to include it in the operational CAMS verification. The transition to operations is being undertaken by CAMS. The preliminary results of the comparisons for the full year and at all reporting stations can be found at the following address: **https://atmosphere.copernicus.eu/charts/cams_surfaer_ver.**

3 DATA ASSIMILATION ACTIVITIES

3.2 4D-VAR ASSIMILATION OF LIDAR PROFILES TO CONSTRAIN VOLCANIC ASK CONCENTRATIONS (RIUUK)

For sudden aerosol events such as volcanic eruptions, uncertainties of emission source parameters impose the characterizing impediment for skillful numerical simulations. In case of volcanic aerosol, the uncertainties of knowledge as important as mass emission rate and plume height can be constrained by assimilation of standard earth observation data. Since the vertical distribution of volcanic aerosol in the atmosphere is highly variable, the application of vertically resolved lidar is one of the most valuable methods to compare observations with model simulations.

In the frame of ACTRIS-2 RIUUK's assimilation activities included the investigation of the information content of ACTRIS-2 lidar backscatter profiles for volcanic ash dispersion re-analyses across Europe. Consequently, the institute's European Air pollution Dispersion-Inverse Model (EURAD-IM) has been extended by modules that enable the use of ACTRIS-2/EARLINET lidar backscatter profiles for 4-dimensional variational (4D-var) data assimilation: new code elements within the pre-processor convert the lidar data from netCDF to PREP format, which is the standard file format read by the EURAD-IM assimilation system. New observation operators that map the model state into the observation space have been developed and tested, allowing on the one hand for the assimilation of volcanic ash assigned lidar profiles and, on the other hand, for the assimilation of lidar profiles, which are not assigned to a specific aerosol species. Two different methods to approach the comparison of lidar backscatter coefficients with model derived aerosol concentrations have been investigated. One observation operator is based on the finding of Ansmann et al. [2012], that a specific way to retrieve estimations of volcanic ash mass concentrations as a function of height is to assume mass specific extinction coefficients. Gasteiger et al. [2011] obtained a mass-extinction conversion factor of 1.45 gm-2 using lidar observations at 532 nm detection wavelength during the Eyjafjallajökull eruption in 2010. According to Ansmann et al. [2012], a lidar ratio of 55 sr was used in the conversion of backscatter into particle extinction coefficients. The other method builds on the calculation of the radiative transfer of the lidar laser signal due to the simulated aerosols in the atmosphere. This is realized by a Mie scattering approach due to Wiscombe [1980], where the different scattering contributions of various aerosol types can be taken into account. However, the Mie theory relies on spherical particle shapes that are not characteristic in case of volcanic ash.

Following the ACTRIS-2 work schedule, the eruption of the Eyjafjallajökull volcano during April and May 2010 was to be analysed as a prototype study, since it depicts a unique special aerosol event. The eruption affected nearly the whole of Europe by enforcing a grounding of air traffic for several days in many countries (e. g. Zehner [2010]). From an assimilation viewpoint, the Eyjafjallajökull eruption is particularly interesting as it poses the challenge of determining highly variable emission characteristics. Furthermore, the Eyjafjallajökull eruption was well observed from many different observation systems. In this way, EARLINET followed the evolution of the volcanic ash cloud over Europe in near real time. Figure 6 shows the locations of all EARLINET lidar stations measuring 532 nm profiles during the Eyjafjallajökull eruption between 14 April and 26 May 2010. In addition to the spatial distance of lidar stations to the volcanic aerosol source, the variability of the observational data quantity as input to the analysis is illustrated by the number of profiles provided in the EARLINET data set per station and day. The sparseness of observations between 28 April and 5 May is related to the weak eruption of the Eyjafjallajökull between the two explosive phases before and after.
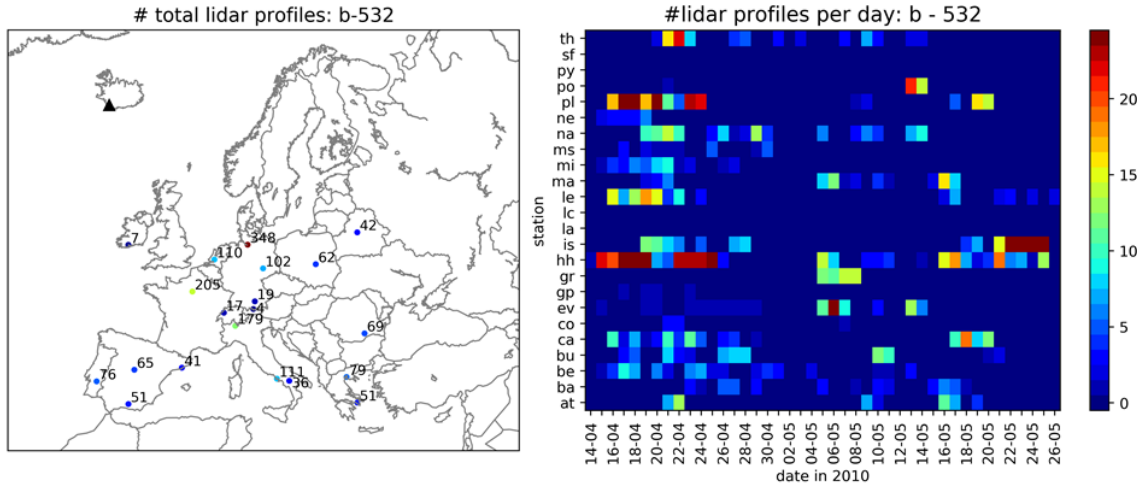
Figure 6. Geographical location of EARLINET lidar stations including number of 532 nm backscatter profiles during the Eyjafjallajökull eruption 2010; the volcano is indicated by the black triangle (left). Daily number of 532 nm backscatter profiles per EARLINET lidar station, tagged by abbreviations (right).

4D-var data assimilation in combination with ensemble modelling can support the estimation of forecast errors and analysis uncertainties. This is of special interest e. g. in case of the investigation of air traffic related threshold values after a volcanic eruption. In this study, all ensemble members are generated by assigning different volcanic ash emission profiles to reflect the uncertainty of the source strengths and injection heights. The wind fields, which are predominantly controlling the ash dispersion, are assumed to be free of significant errors, such that all ensemble members are driven by the same meteorological WRF forecast. Notably, the ensemble is designed to reflect the highest applicable extent of the eruption scenario, consisting of nine ensemble members that are chosen to include the potential extremes of the eruption strengths and heights, and possible emissions in between. Besides the EARLINET profiles, some experiments utilized CALIOP extinction profiles and SEVIRI volcanic ash column mass loading retrievals in the assimilation as additional operational background information source. These experiments are described in detail in Lange (2018).
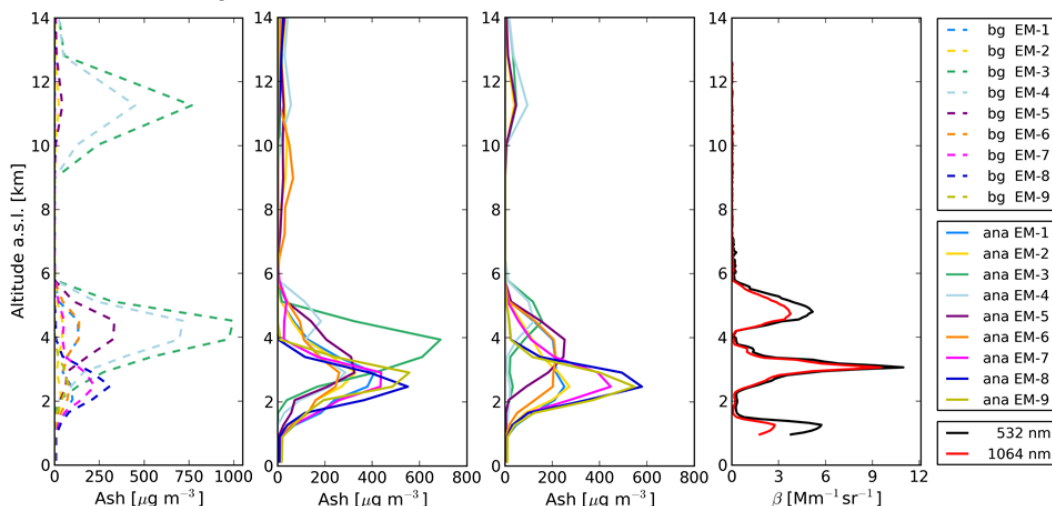

Figure 7. Vertical volcanic ash distribution over Leipzig on 16 April at 13 UTC: Concentration profiles of the background (left), the analysis using SEVIRI retrievals (2nd from left), the analysis applying combined SEVIRI and CALIOP retrievals (3rd from left), and the lidar retrieved mean backscatter coefficient profiles at 532nm and 1064nm of the Leipzig EARLINET station (right).

Figure 7 shows the modeled vertical ash concentration profiles of the 4D-var ensemble's background and analyses fields on 16 April 2010 at 13:00 UTC. The background simulations of ensemble member (EM) 3 and EM-4 contain two ash layers between 2–6 km and 9–13 km, while the formation of the upper ash layer is suppressed in both analyses. Regarding the background states, all nine ensemble members feature ash layers at altitudes varying between 1 km and 6 km and differing in ash concentrations between 43 µg m−3 to 996 µg m−3. In both analyses, the ensemble spread decreases, such that eight ensemble members approximately concur that the ash cloud contains its highest concentration at about 2–3 km height. The comparison of the analyses and lidar profiles attained by the EARLINET lidar station in Leipzig supports the conclusion that all ensemble members of both analyses represent the volcanic ash layers in the correct vertical range.
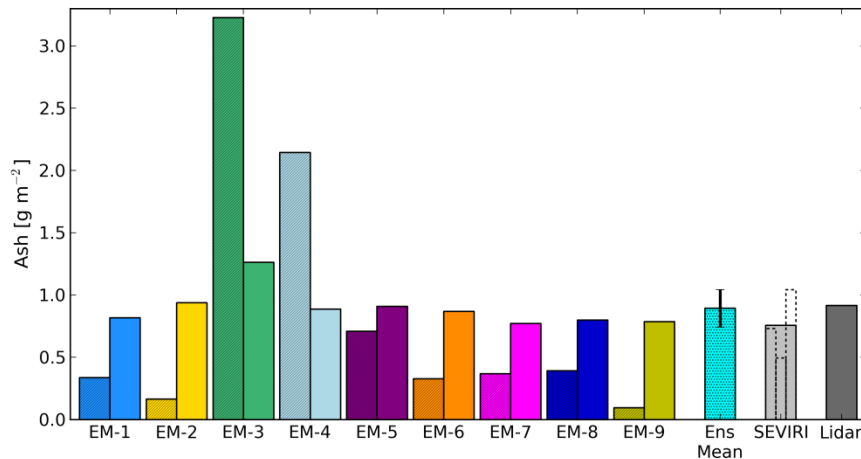

Figure 8. Volcanic ash column mass loads at the EARLINET station in Leipzig on 16 April at 13 UTC: background (shaded bars – left) and SEVIRI analysis (clear bars – right) of the 4D-var ensemble, the analysis ensemble mean (Ens Mean, cyan dotted) including the standard deviation (error bar), SEVIRI observation mean (light gray) calculated from three retrieved pixels included in the considered model grid cell (dashed clear bars), and lidar derived mass loading equivalent (dark gray).

Figure 8 combines the mass column loadings obtained from ensemble forecasts, analyses, three SEVIRI pixels, and lidar measurements for the EARLINET station in Leipzig on 16 April at 13:00 UTC. The bar chart includes the column values from the background and analysis simulations of all nine 4D-var SEVIRI ensemble members, as well as the ensemble mean analysis, the mean of SEVIRI observations, and the mass loading equivalent derived from the EARLINET lidar observations. Reflecting initial uncertainty the background simulations reveal large differences in the column value between the ensemble members. The analysis column mass loadings illustrate much better agreement, whereas the mean column mass loading of all nine ensemble analyses accounts for 0.89 g m−2. For comparison with observational data, the column mass loading of the SEVIRI retrievals and the column mass loading equivalent of the 532 nm lidar observations are illustrated. An ideal ensemble prediction system shows a perfect relationship between ensemble spread and ensemble mean error (Grimit and Mass [2007]). Regarding the ensemble analysis of volcanic ash column mass loadings, this objective is well fulfilled. SEVIRI and lidar derived column values of 0.76 g m−2 and 0.92 g m−2, respectively, lie within the ensemble spread of the 4D-var ensemble analysis. Thereby, the deviations between the mean analysis and observations remain small, as desirable in case of poor a priori knowledge of emission strengths.

Finally, the following conclusions can be drawn for this project work, which is certainly dependent on the limits of the selected case study: The 4D-var ensemble analysis sustains the long-range transport of volcanic ash from Iceland beyond Central Europe. Regarding the observability of the aerosol dispersion above Europe, the 4D-var ensemble performs well to determine the impact of the observational information. A final judgment on the general impact of ACTIRS-2 lidar backscatter profiles on the full aerosol load is of course not representative based on this single case study of the Eyjafjallajökull eruption. It is most likely

ACTRIS (www.actris.eu) is supported by the European Commission under the Horizon 2020 – Research and Innovation Framework Programme, H2020-INFRAIA-2014-2015, Grant Agreement number: 654109

Page **12** / 30

that the large fragmented cloud cover above Europe impaired not just the EARLINET measurements but also the SEVIRI and CALIOP observational data and hence, affected the observability analyses. However, the study demonstrated a significant contribution of the information about the vertical distribution of aerosol in the atmosphere by lidars, which cannot be provided by any other observations that have the capability of operationalization and that are organized in continent-wide networks.

3.2 USE OF AN ENSEMBLE KALMAN FILTER TO IMPROVE THE VERTICAL REPRESENTATION OF DUST (BSC)

The vertical structure of dust plumes needs to be better represented in model simulations (Binietoglou et al., 2015). High uncertainties in the representation of dust vertical structure have implications for the radiation's budget calculations and model aerosol transport. Yet, modelled vertical structures are generally poorly constrained by observations. BSC's data assimilation activities aim to tackle the difficulties in constraining dust information in the vertical, making use of model simulations from the chemical weather prediction system NMMB-MONARCH, formerly known as NMMB/BSC-Dust (Perez et al., 2011), enhanced with data assimilation capability. Below we summarize the activities carried out to solve three case studies: (i) a case study related to measurements taken in Senegal (which was part of the initial report on assimilation activities, D13.4), (ii) a case study related to measurements from different sites located in the East Mediterranean region, and (iii) a case study using measurements from the EARLINET/ACTRIS summer 2012 intense observational period. The latter two case studies have used a more refined implementation of the observation operator and of the treatment of the observations compared to the preliminary settings used for the former one.

3.2.1 Dust model

We have used for our simulations the dust component of the NMMB-MONARCH chemical weather prediction system. The overall system consists of gas-aerosol modules fully online integrated with the NMMB meteorological model (Janjic and Gall, 2012) from the Unites States National Centers for Environmental Prediction (NCEP). Different dust schemes are implemented in NMMB-MONARCH. In the first case study, we have used the dust emission scheme as described in Perez et al. (2011). This scheme follows the empirical relationship of Marticorena and Bergametti (1995) and Marticorena et al. (1997) according to which the vertical dust flux is proportional to the horizontal saltation flux. The latter is simulated according to White (1979), and is proportional to the third power of the wind friction velocity. A particle-diameter dependent threshold of the friction velocity, including a correction for soil moisture, determines the velocity above which the soil particles begin to move in saltation. In the other two case studies, we have used the GOCART dust emission scheme (Ginoux et al., 2001), which estimates dust emission based on horizontal wind speed at 10m and a topographic source function representing areas where sediment is likely to have accumulated, making it available for wind erosion. NMMB-MONARCH uses a sectional approach for the transport of particles, i.e. the dust size distribution is decomposed into size bins. The total vertical mass flux is distributed among the dust bins according to a specific dust size distribution at sources. The first case study has used a distribution over sources derived from D'Almeida (1987), which assumes that the vertical dust is size distributed according to three lognormal background source modes. The other two studies have used the size fractions given in Ginoux et al. (2001).

An ensemble of model simulations is generated for data assimilation purposes. Each ensemble member is run with perturbations of model parameters which are deemed to be particularly uncertain in the dust emission scheme. The ensemble is created by perturbing the vertical flux of dust in each of the eight dust bins, and imposing some physical constraint on the perturbations. This is equivalent to perturbing the total vertical flux as well as its size distribution at sources. Additionally, we have perturbed the threshold velocity for dust emission. This considers the uncertainty of the model with respect to both surface winds and soil humidity. The structure of our source perturbations, for both types of perturbations, is temporally and spatially constant. The spin-up period for the ensemble ensures that perturbations applied at the sources propagate everywhere in the simulation domain.

3.2.2 Data assimilation scheme

NMMB-MONARCH has been coupled with an ensemble-based data assimilation technique known as Local Ensemble Transform Kalman Filter (LETKF; Hunt et al., 2007). For this purpose, a 12-member forecast ensemble based on known uncertainties in the physical parametrizations of the mineral dust emission scheme has been created as described in the previous section. The main developments for the enhancement of the NMMB-MONARCH with a data assimilation capability are described in Di Tomaso et al. (2017). Here, we will describe additional features that have been added, or are particularly relevant, to deal with profile observational information. The sparse nature of lidar ground-based observations is better handled with reasonably high-resolution simulations, which are more efficiently run on a regional, rather than a global, domain. Therefore, the data assimilation scheme, initially built for a global regular grid, has been adapted to the NMMB-MONARCH regional rotated coordinate system. The rotated frame is used in order to reduce the variation of the grid size.

Subsequently, the observation operator H has been built for ground-based extinction profiles at 532 nm. H consists in calculating the model equivalent of the observations., i.e. to map the ensemble mean state vector into the observation space. Hence it has two components: the vertical and the horizontal interpolation component, followed by the calculation of an extinction profile from a model mass concentration profile.

The simulated extinction in m-1 at a given wavelength λ is calculated at a given observation location according to the following linear operator:

$$ext_\lambda = \sum \frac{3 qext_\lambda C_b}{4 r_b \rho_b} \quad (1)$$

where ρ_b [kg m−3] is the particle mass density, r_b [m] is the effective radius, C_b [kg m−3] is the dust mass concentration for each dust bin, and $qext_\lambda$ is the extinction efficiency factor. The extinction efficiency factors for 532 nm have been calculated either using the Mie scattering theory (Mishchenko et al., 2002) assuming dust spherical particles, or making a non-spherical particle assumption (depending on the case study). Particles are assumed non soluble, and modelled for the 8 model size bins, and, within a bin, a lognormal distribution for dust with geometric radius of 0.2986 μm and standard deviation of 2.0. We have used information on refractive indices at different wavelengths from the OPAC database (Hess et al., 1998). The imaginary part of the refractive index has been interpolated from the available values at 500 and 550 nm. Extinction efficiency factors for NMMB-MONARCH 8 bins are estimated as 1.489289, 3.438292, 3.109589, 2.458298, 2.251090, 2.253891, 2.149677, 2.1017. In our future work, we plan to revise our choice of optical properties since the OPAC database is known to provide a too absorptive dust aerosol (Kaufman et al., 2001). An ensemble averaged extinction efficiency is calculated during the assimilation as in Schutgens et al. (2010) as an average of the extinction efficiency of the individual bins weighted by the bin mixing ratios. We use a 24-hour assimilation window and observations are considered for assimilation either at four time slots within the window, at 0, 6, 12 and 18 UTC (first two case studies) or at every hour, at 0, 1, ⋯, 23 UTC (third case study). The system uses as first guess a 1-day forecast with output every 6 or 1 hour. Simulated observation and background departures are calculated at each time slot. We are using the LETKF implementation with a four-dimensional extension as described in Hunt et al. (2007). The state vector comprises of the mixing ratio at all the time slots considered. Background observation means and perturbation matrices are formed at the various time slots when the observations are available. They are then concatenated to form a combined background observation mean and perturbation matrix which are used for the standard LETKF calculations, i.e. the analysis increments are based on all innovations throughout the day. No inflation of the ensemble spread has been used in the first two case studies.

Vertical and horizontal localization are performed through R-localization, i.e. the localization is performed in the observation error covariance matrix, making the influence of an observation on the analysis decay gradually toward zero as the distance from the analysis location increases. To achieve this, the observation error is divided by a distance dependent function that decays to zero with increasing distance, $e^{\frac{-d^2}{l^2}}$, where d is the distance in the grid space between an observation and the model grid in which the analysis is calculated, and l is horizontal or vertical localization factor. As an example, when using a

horizontal localization factor equal to 2, the observation's influence in the horizontal plane becomes negligible at distances greater than 3 to 4 grid points (the actual distance is resolution dependent). We apply both horizontal and vertical localization. We have used a vertical localization factor equal to 1 in all our simulations. This means that after two grid points the influence of an observation in the vertical direction becomes negligible. The value for the localization factor has been varied from 4 to 8 in the different simulations that we have performed, more details are given in the following sections.

3.3.3. Observational data

a) Senegal case study
Profile observations were provided by the University of Lille for the M'bour site outside Dakar, in Senegal, for case studies of dust intrusions observed with a multi-wavelength Mie-Raman lidar (Bovchaliuk et al., 2016, and Veselovskii et al., 2016). The spectral extinction profiles are provided at two wavelengths: 355 nm, and 532 nm for a profile of range of signal. However, we have assimilated only profiles at 532 nm. Observation height h is calculated from the range s of the signal with h=s*cos(46.5°). All the extinction profiles are computed by averaging 2-hour lidar signals except when some of the measurements are not available. All the night time extinction profiles are derived from the Raman method, while the daytime extinction profiles are calculated from the Klett method. The assumed lidar ratio that is required for the Klett method is taken from the nearest night time Raman retrieval. Due the overlap range of the lidar system, only signal above 700 m (in height) is considered valid. For this reason, only observations above 700 m are used for data assimilation.

b) East Mediterranean case study

We have used profile observations from an event of dust transport towards the East Mediterranean occurred during April 19-23 2017. This event was observed by 3 lidar sensors located in Finokalia (Crete), Limassol (Cyprus) and Haifa (Israel) part of PollyNet (http://polly.tropos.de/), a network of portable Raman-polarization lidars operated mostly within the framework of EARLINET/ACTRIS. Data have been processed to retrieve dust extinction coefficient profiles by the ground-based remote sensing group of the TROPOS institute, together with an uncertainty estimation. Only valid signal was provided, so overlap issues of lidar were excluded a priori. Figure 9 shows the uncalibrated attenuated backscatter coefficient at 1064 nm and the volume depolarization ratio for the period of the case study at the Limassol site.
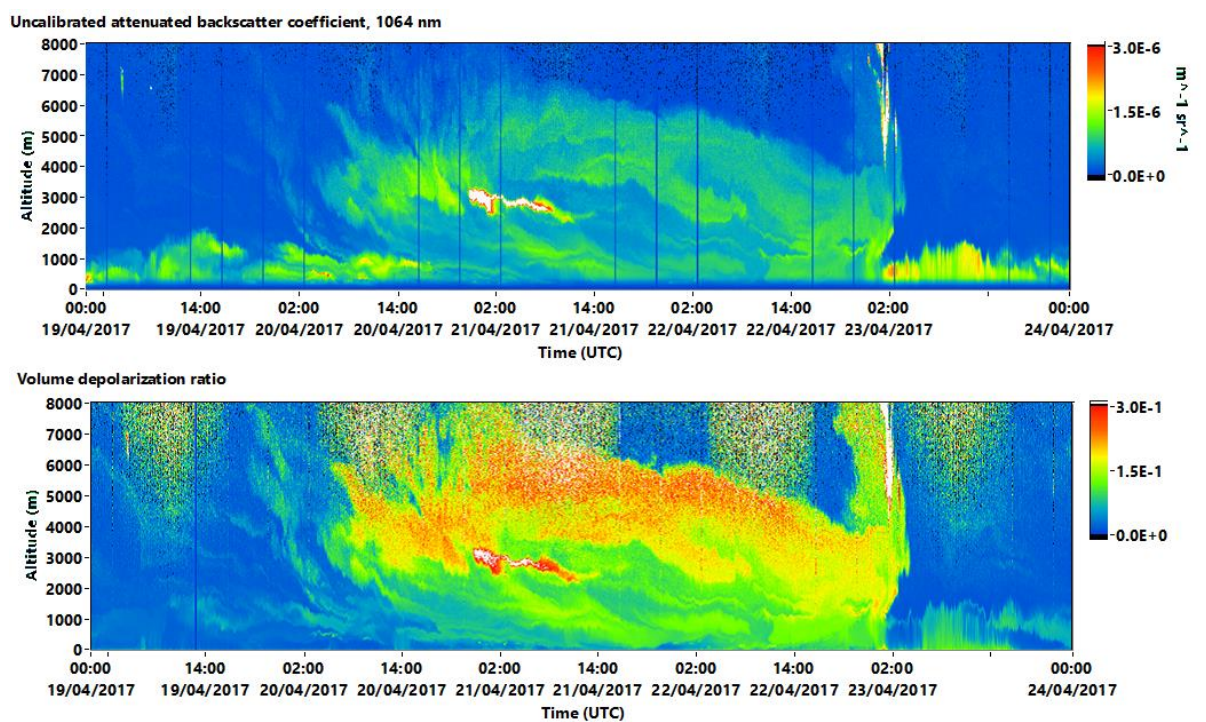
Figure 9. Uncalibrated attenuated backscatter coefficient at 1064 nm (top) and the volume depolarization ratio (bottom) at the Limassol (Cyprus) site, for a dust intrusion occurring on April 19-23 2017.

c) EARLINET/ACTRIS summer 2012 case study

We have used dust profiles derived from measurements during the ACTRIS summer 2012 campaign, more specifically from the period 9-12 July 2012 (Sicard et al., 2015). We have used data from three EARLINET stations: Bucharest (bu), Granada (gr), and Potenza (po). Lidar observations have been processed through the Single Calculus Chain (SCC), the centralized processing tool developed within EARLINET/ACTRIS for the harmonized processing of the aerosol lidar measurements (D'Amico et al., 2015, Mattis et al., 2016). Aerosol backscatter, extinction and depolarization ratio profiles obtained as standard products from SCC have been post-processed by the CNR-IMAA institute by applying the POLIPHON algorithm (Ansmann et al., 2011) to retrieve the dust backscatter coefficient profiles together with the uncertainty estimate. Dust extinction coefficient profiles have been then derived by multiplying the backscatter coefficients by a constant lidar ratio (55 sr; Papagiannopoulos et al., 2018). Observation uncertainty has been inflated by 12% to take into account the assumption made in the latter conversion.

3.3.4 Data assimilation experiments

a) Senegal case study

We have run a lidar assimilation experiment for the dust event that occurred on March 30-31 2015 in the Dakar region. The simulation domain is the one shown in Figure 10. Simulations were run with 40 hybrid pressure-σ layers, and a horizontal resolution of 0.33° by 0.33°. We have assimilated observations from model level 7 to 17, i.e. above 700 m and up to circa 4000 m. LETKF has the advantageous feature that it applies localization, i.e. it performs the analysis locally. At each grid point only observations within a 4 grid point distance (i.e. 1.3° circa) were assimilated. The observation vertical information is interpolated at the mid altitude of the model layers using a third-order polynomial interpolation function. Model tracers are then interpolated at the observation location at each model level. We have used an observation uncertainty described by the diagonal observation error covariance matrix with elements equal to 0.0001+0.01*ext532.

We have run a free ensemble simulation, without assimilating any observation, starting on mid-February 2015 from a deterministic control experiment, to spin-up the ensemble before data assimilation. The spin-up period for the ensemble ensures that perturbations applied at the sources propagate everywhere in the simulation domain. Figure 10 shows the dust aerosol optical depth (AOD) analysis at 550 nm at three time steps of the assimilation window. The corresponding analysis increments are shown in Figure 11. For this particular event the assimilated profile corrects an underestimation in total column extinction in the model. Though observations were available only at 18 UTC, the 4D extension used for the LETKF propagates the observational impact through the whole assimilation window.
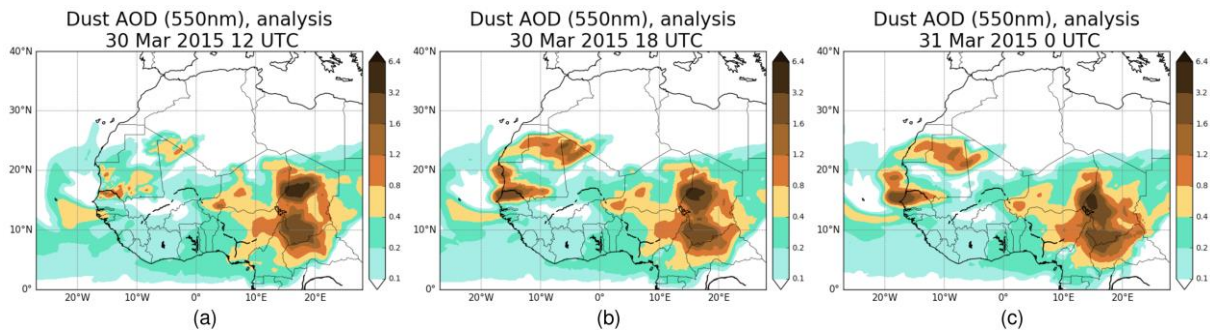

Figure 10. Dust AOD analysis at 550 nm at three time steps of the assimilation window produced by the assimilation of a lidar extinction profile at the M'Bour site in Senegal. The profile was measured on 30 March 2015 at 18 UTC.
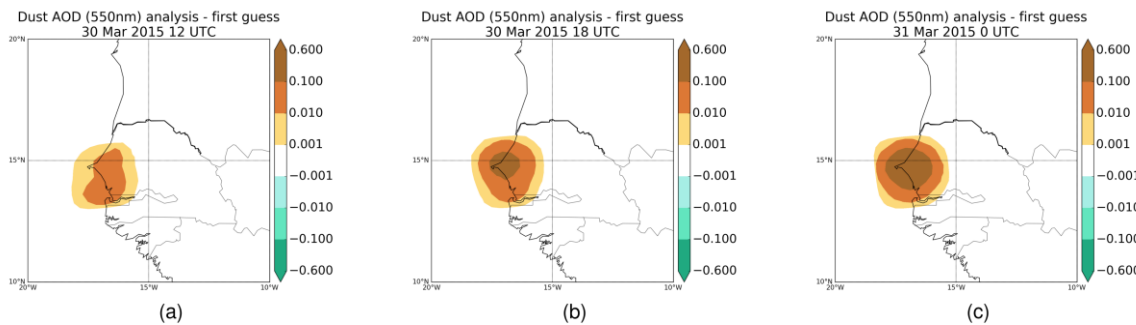

Figure 11: Analysis increments (analysis – first guess) corresponding to the three analyses of Figure 10.

Figure 12 shows the extinction profiles at 532 nm at the lidar site location for the model first guess, the analysis, and, when available, for the observations at three time steps of the assimilation window. As a sanity check we can note that the analysis is closer to the assimilated observations than the first guess (Figure 12b).
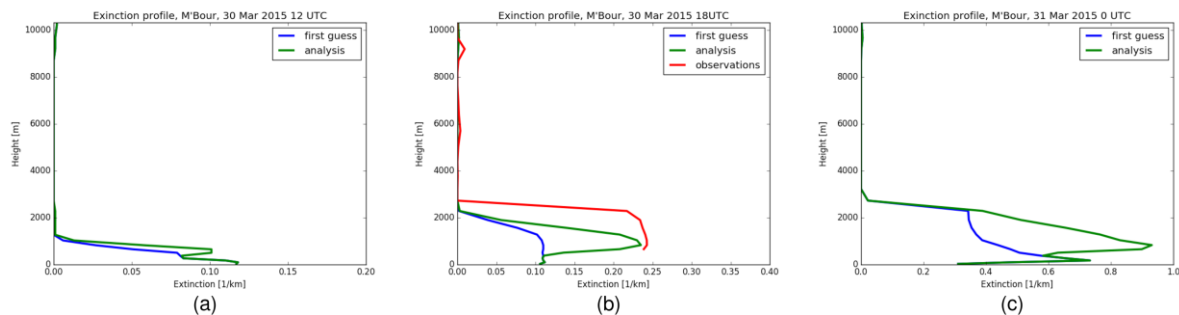
Figure 12: Extinction profiles at 532 nm for the model first guess (blue), the analysis (green), and, when available, for the assimilated observations (red) at the M'Bour site at three time steps of the assimilation window.

b) East Mediterranean case study

We have run further assimilation experiments and over a wider domain for the dust event occurring on April 19-23 2017. The simulation domain is the one shown in Figure 13. The extension of the domain was chosen to cover all the main source areas that have contributed to the dust transported over the measurements sites. Dust emitted in North Africa and in the centre of Sahara has been transported towards the East part of the Mediterranean basin. The extent and dynamic of the event can be observed as predicted by the NMMB/BSC-Dust model (https://dust.aemet.es/forecast) or by the models taking part in the WMO Sand and Dust Storm Warning Advisory and Assessment Syst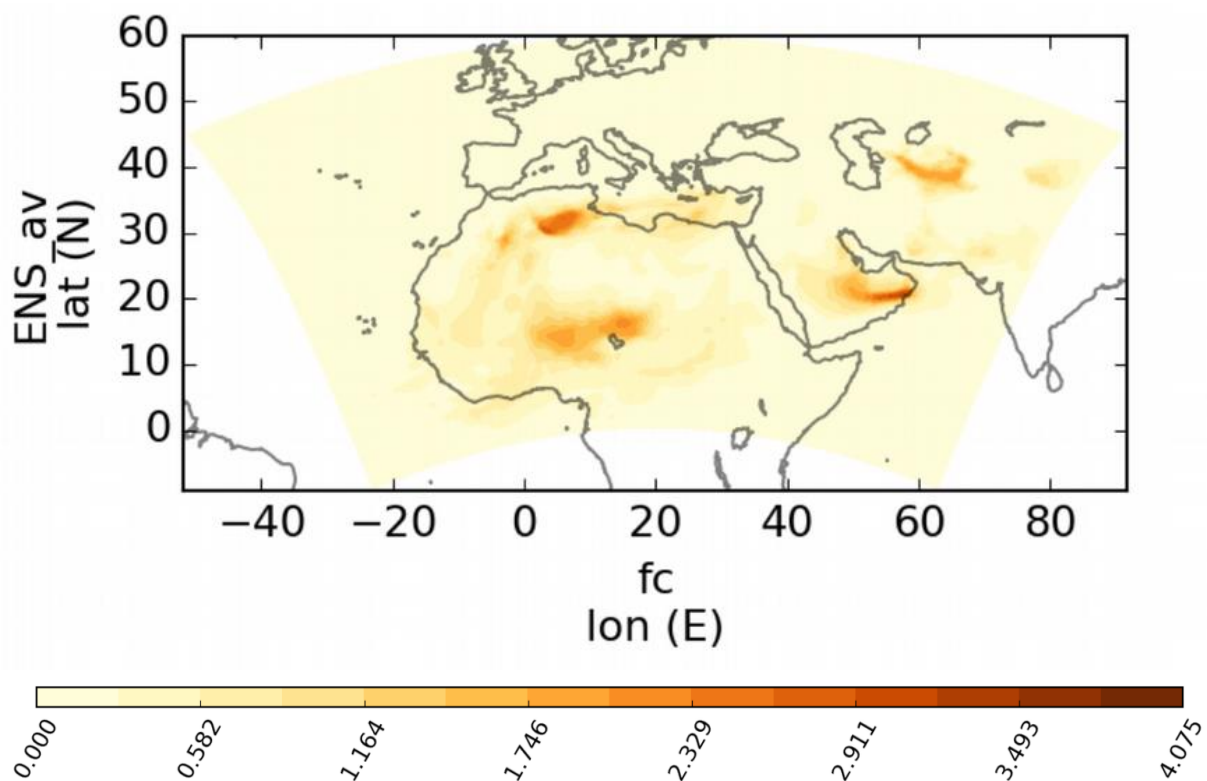em (SDS-WAS; Terradellas et al., 2015) forecast comparison (https://sds-was.aemet.es/forecast-products/dust-forecasts/forecast-comparison).

Figure 13: Mean ensemble forecast for April 20 18Z.

Simulations were run with 40 hybrid pressure-σ layers, and a horizontal resolution of 0.33° by 0.33°. We have assimilated observations below 10km. At each grid point only observations within a 24 grid point distance and with a value 8 of the horizontal localization factor were assimilated. The uncertainty of the assimilated data is 0.5 the uncertainty estimated by the remote sensing team. Also, a minimum value of 10-6 for the uncertainty was set, in order to avoid an analysis biased toward zero, because the observational errors are smaller for smaller values of the extinction coefficient. Observations were interpolated to the model hours (0, 6, 12 and 18 UTC) only when the mean timestamp of the observations was within ±1.5 hour from the model time. When two or more observations belong to the same time window, the assimilated profile has been weighted according to their relative contribution in terms of temporal coverage (in the overlap between the 3 hour window and the observation initial minus end times). Errors are interpolated assuming a Gaussian correlation length of 36 hours for each vertical lidar layer. The observation profiles

are interpolated at the models heights, and the errors are estimated assuming a Gaussian correlation with a length scale of 1 km within all the lidar data for each model layer.

We have run a free ensemble simulation, without assimilating any observation, starting on April 1 2017 to spin-up the ensemble before data assimilation. As stated earlier, the spin-up period for the ensemble ensures that perturbations applied at the sources propagate everywhere.

Figure 14 shows the ensemble mean first guess (left) and the ensemble mean analysis (centre) obtained by assimilating observations of the 3 lidar profiles (when available) at three different simulation times over the period of study. Negative values of the analysis increments (analysis minus first guess, right plot) indicate that, for this particular event, the assimilated profiles correct an overestimation in total column extinction in the model. Figure 15 shows the extinction profiles for the model first-guess, the analysis and the observations at each lidar site for one of the simulation times shown in Figure 14. Consistently with the increment plots, this figure shows an overall correction of a model underestimation of the total column extinction. Furthermore, assimilated observations are able to correct in most cases the plume height.
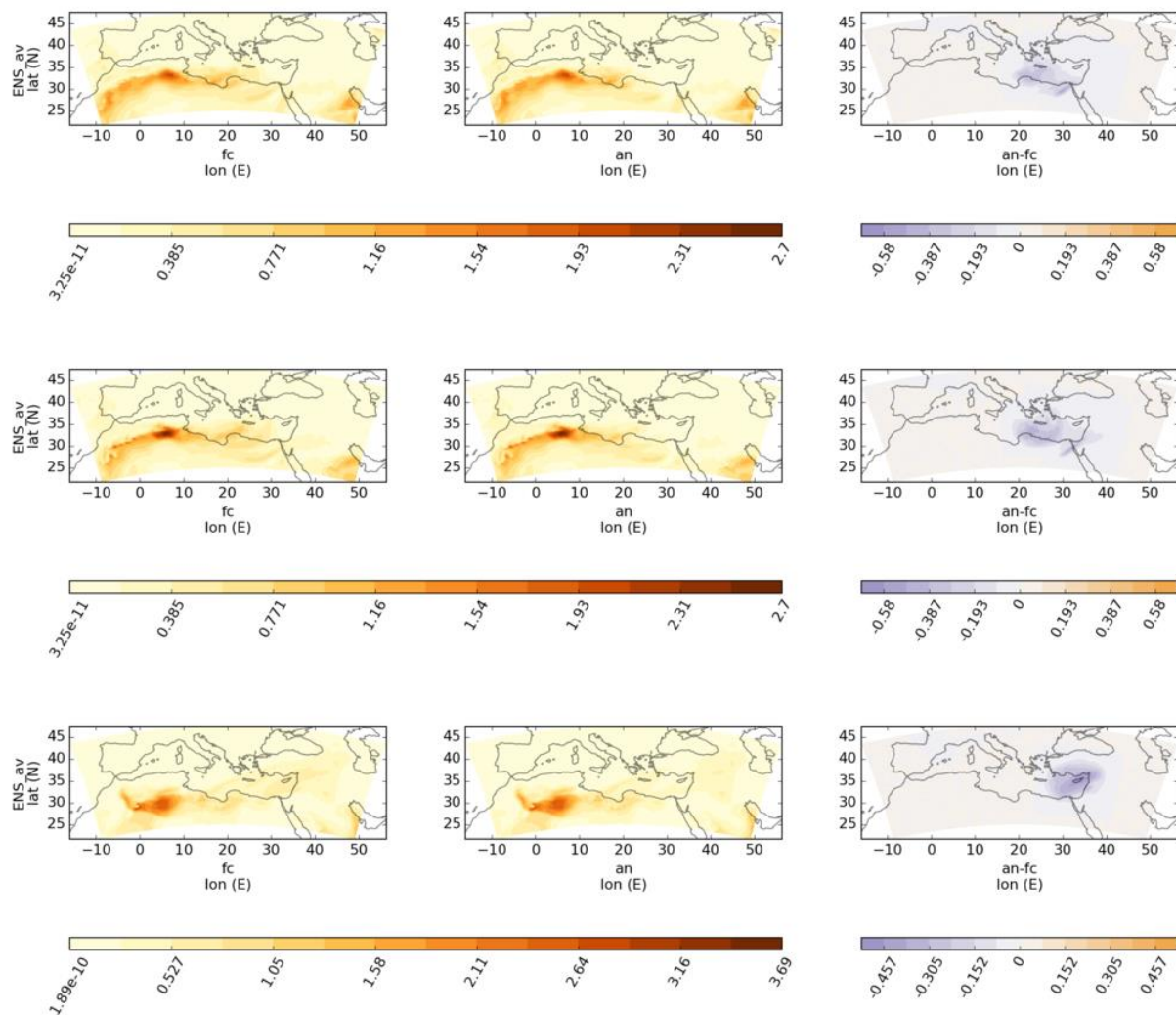

Figure 14: Mean ensemble forecast (left), mean ensemble analysis (centre), increments (right) on April 19 at 18Z (top), April 20 at 0 UTC (centre) and April 21 18 UTC (bottom) 2017.
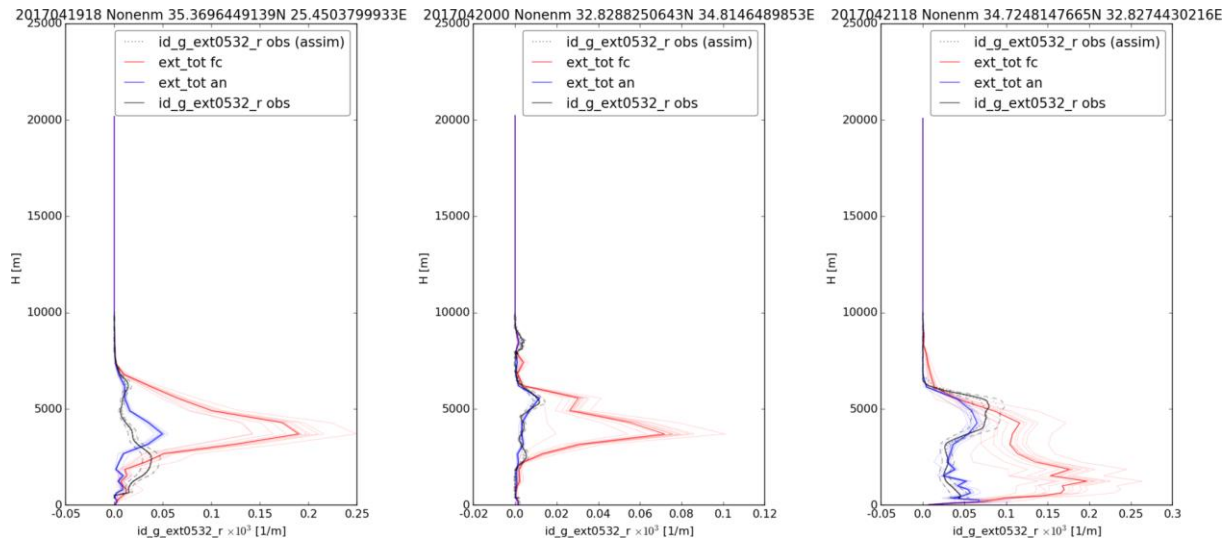
Figure 15. Extinction vertical profiles for the ensemble forecast (red), the ensemble analysis (blue) and the observations (black) at Finokalia on April 19 at 18 UTC (left), at Haifa on April 20 at 0 UTC (centre) and at Limassol on April 21 at 18 UTC (right). Bold lines for model profiles indicate ensemble mean values, while thin lines indicate ensemble member values. Observation uncertainty is depicted with dashed black lines. The altitude 0 is the value of the model surface topography

c) EARLINET/ACTRIS summer 2012 case study

Simulations were run with 40 hybrid pressure-σ layers, and a horizontal resolution of 0.66° by 0.66°. Meteorological reanalyses (ERA-Interim) were used to initialize the meteorology at the start of every forecast (at 0 UTC) and as boundary conditions every 6 hours of the forecast. A value of a 6 grid point distance (~4 degrees) has been used for the horizontal localization factor (determining the extent of the radius of influence of an observation in the horizontal plane), a vertical localization factor equal to 1 and a time localization of 4 hours. Because of the need of an internal balance between the background and observational error covariance matrices in the data assimilation procedure, the uncertainty of the assimilated observations is 0.5 the uncertainty estimated by the remote sensing team (i.e., the observational error variance is multiplied by a factor 0.25), while the ensemble covariance matrix has been inflated with a factor of 1.1. As for the previous case study, a minimum value of 10-6 for the uncertainty was set. The assimilation is run using a higher time resolution compared to the previous two case studies. We considered a 1 hour time resolution for the analysis calculation within a 24 hour assimilation window. Observations were interpolated to the model hours only when the mean timestamp of the observations was within ±30 minutes from the model time. When two or more observations belong to the same time window, the assimilated profile has been weighted according to their relative contribution in terms of temporal coverage (in the overlap between the 1 hour window and the observation initial minus end times). Errors are interpolated assuming a Gaussian correlation length of 36 hours for each vertical lidar layer. The observation profiles are interpolated at the model heights, and the errors are estimated assuming a Gaussian correlation length of 1km within all the lidar data for each model layer. While for the previous two case studies dust particles are assumed spherical in the calculation of the extinction efficiency factors, here a non-spherical assumption is made. We have run a free ensemble simulation, without assimilating any observation, starting on June 2012 to spin-up the ensemble before data assimilation. Figure 16 shows the ensemble mean first-guess (left) and the ensemble mean analysis (centre) obtained by assimilating observations of the 3 lidar profiles (when available) at a given time (July 10 2012 at 22Z) during the study period.
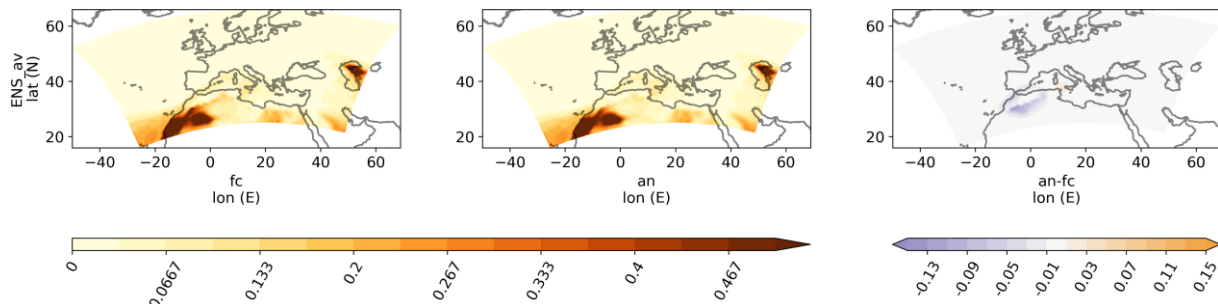
Figure 16. Mean ensemble forecast (left), mean ensemble analysis (centre), increments (right) on July 10 2012 at 22Z for a selected part of the model domain. Colorscale is truncated to the shown values (0 to 0.5 on the left and centre panels, -0.15 to 0.15 on the right) for clarity.

Negative values of the analysis increments (analysis minus first guess, right plot) in Northern Africa indicate that, in this assimilation step, the assimilated profiles correct an overestimation in aerosol optical depth (AOD) in the model. At a lower extent, an underestimation in AOD is corrected over the Sea of Sicily and Tyrrhenian Sea. The analysis corrections are relatively small in terms of AOD. However, it is interesting to analyse whether the lidar observations are able to constrain the vertical structure of the dust plume.

Figure 17, 18 and 19 show assimilated lidar observations and simulated observations at the three lidar locations: Bucharest, Potenza and Granada respectively. Changes in the analyses compared to the forecast are due to the local assimilated observations but also to changes in the dust plume due to analyses increments caused by the assimilation of the other two lidars present in the study domain. We considered cloud-screened and quality-assured (Level 2.0) direct-sun AOD retrievals between 440 and 870 nm. AERONET AOD at 550 nm was obtained using the Ångström law. Large differences between the lidar column integrated extinction and AERONET optical depth at the Bucharest station are likely due to the presence of non-dust aerosols. A lower top layer of dust in the analysis compared to the forecast, and in agreement with the observations, can be observed at the Bucharest station at day two and three of the experiment (days 10 and 11 of July). Some reduction of the dust extinction in the analysis at the Potenza station in day one, and partially day two, are due to some zero (or close to zero) value lidar profiles. As for the Bucharest station, the analysis show a lower dust top layer compared to the forecast, in particular towards the last day of the experiment. From a first qualitative assessment the analysis shows a good agreement with the lidar column integrated extinction at the Granada station. Optical depth from three different AERONET stations (Granada, Malaga, Cerro Poyos) are shown since they are within a one degree distance from the lidar location.
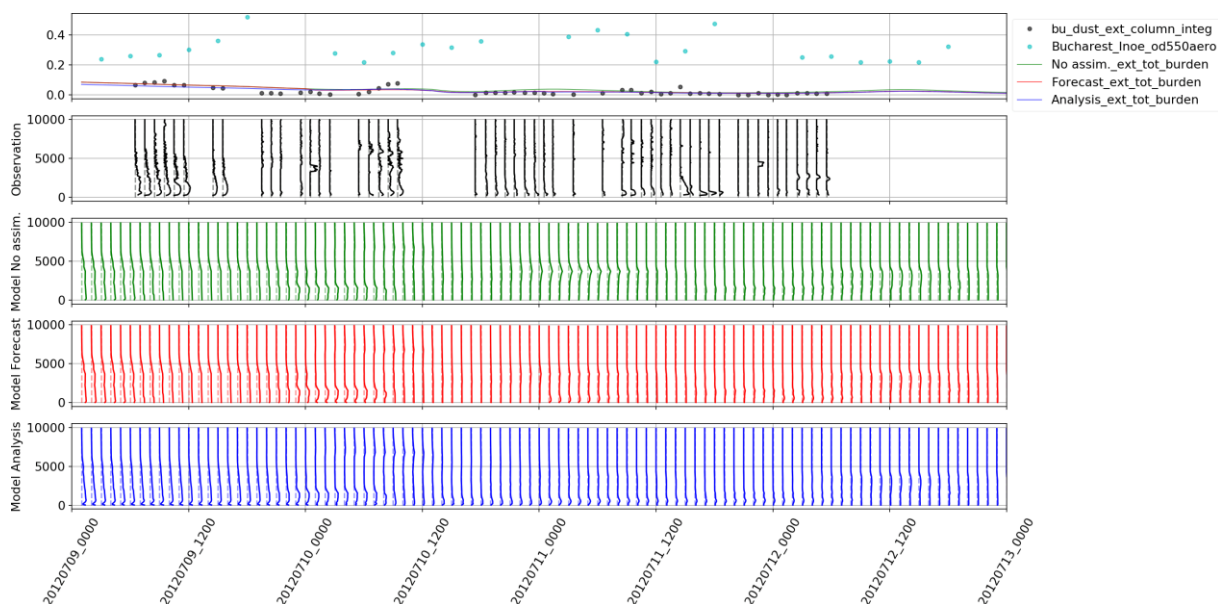
Figure 17. Aerosol optical depth (AOD) at 550nm at a local AERONET station (Bucharest INOE; cyan), column integrated extinction of lidar dust profiles (lidar equivalent AOD, black), extinction total burden of analysis (analysis equivalent AOD, blue), analysis-initialized forecast (AOD, red), forecast with no assimilation (AOD, green) at 532nm for the experiment period, from 9 July 2012 to 12 July 2012 (top panel). Lower panels contain dust extinction profiles from assimilated lidar observations (black), from a simulation without data assimilation (green), from model forecast initialized from an analyses (or first-guess; red), from model analysis (blue). The vertical coordinate for the latter is altitude (m) above the surface, and the horizontal scale is the same for all the profiles in this figure.
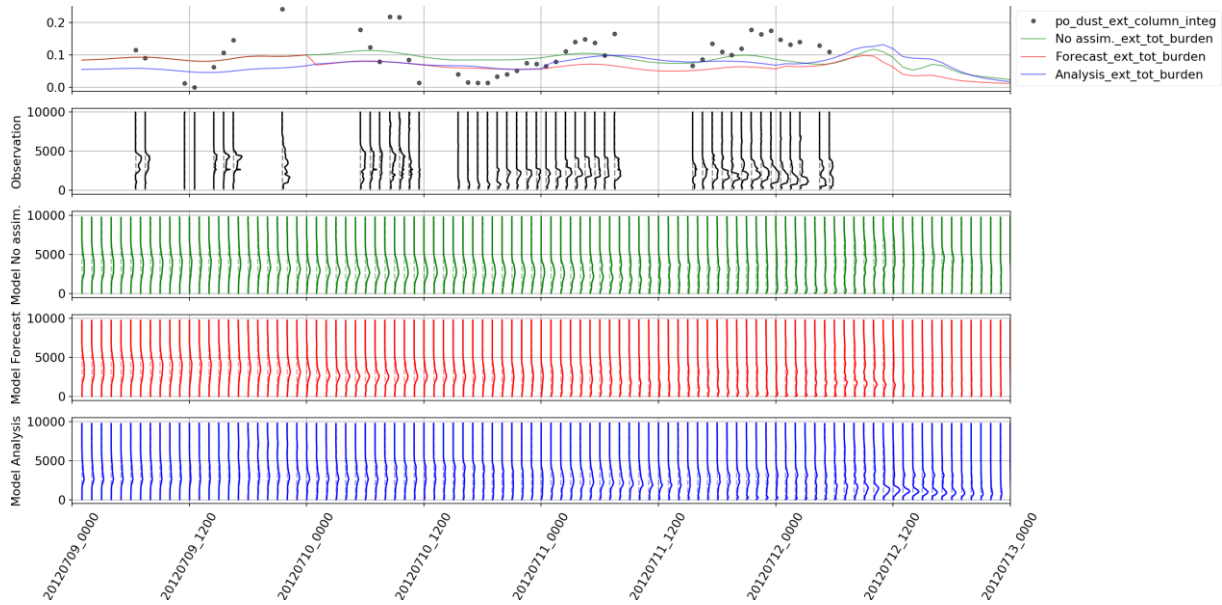

Figure 18. As in Figure 17, but for the Potenza lidar. No AERONET measurements reported in the top panel for this station.
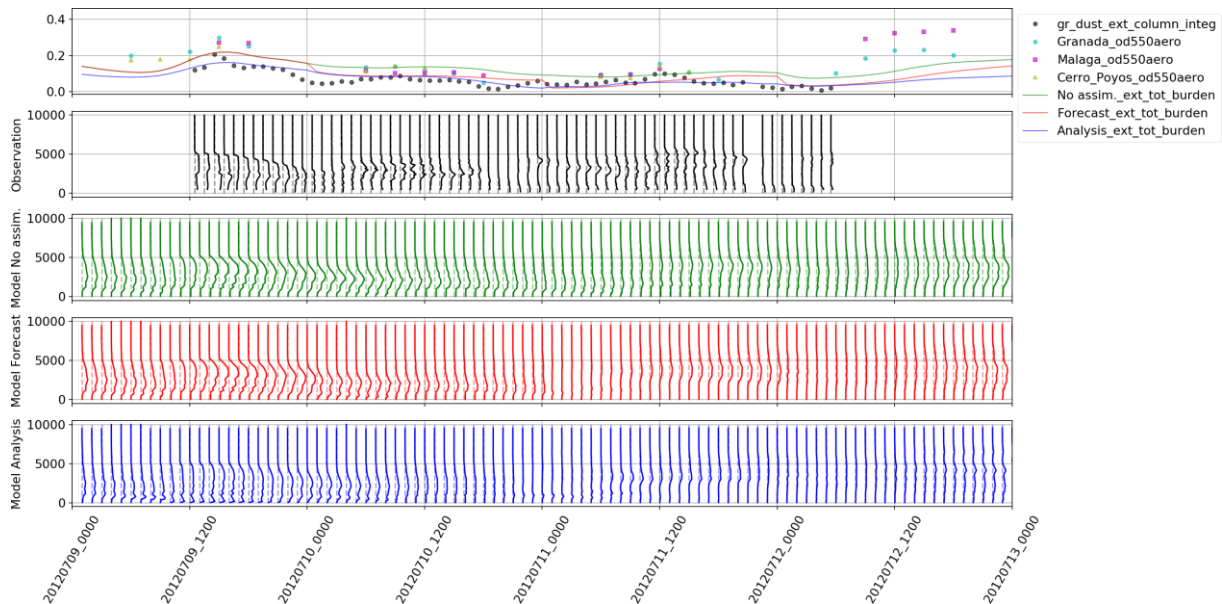

Figure 19. As in Figure 17, but for the Granada lidar, and with measurements reported from three AERONET stations (Granada, Malaga and Cerro Poyos) reported in the top panel.

Small differences between the lidar column integrated extinction and AERONET optical depth at the three stations are, also in this case, likely due to the presence of non-dust aerosols, and partially to not having a

lidar valid signal at the lowest altitudes. The forecast (or first-guess) is equivalent to the forecast of the no-data assimilation experiment only in the first day of the experiment. It is closer to the analysis during the first hours of the forecast (as expected by the analysis initialization) and closer to the no-assimilation experiment towards the end of the forecast window (drifting towards its own climate). The forecast is initialized every day of the experiment both for the meteorology and for the dust concentrations. The analysis shows a lower dust top layer compared to the forecast in the first day of the experiment, a more flat profile during the second day of the experiment, and a reduction of dust extinction in the third and fourth day of the experiment, in agreement with the assimilated observations. Overall the assimilation of three lidar profiles helps in correcting inconsistencies between observed and simulated dust plumes.

3.3. ASSIMILATION OF AEROSOL BACKSCATTER PROFILES IN AN OPERATIONAL 4D-VAR SYSTEM (ECMWF)

3.3.1 Data assimilation experiments.

The ECMWF/CAMS system described in section 2.2 routinely assimilates observations of AOD. This component has a high level of maturity both in the operational model and in the assimilated products. The accuracy of AOD is high due to the fact that it is a column integrated quantity. However, the vertical distribution of the aerosol fields, particularly in the case of aerosol plumes of volcanic origin is not always realistic. In order to address this issue, the assimilation of profiling parameters such as lidar backscatter or extinction has been explored to give a better accuracy on the vertical description of the aerosol in the ECMWF model.

In 2012, preliminary studies showed the feasibility of assimilating the attenuated backscatter from CALIOP (Benedetti and Dabas, 2016). The assimilation of the lidar data provided positive impacts on the description of the aerosol vertical distribution but created a bias on the AOD visible on the comparison with AERONET data. Since the lidar assimilation was introducing a degradation of the main aerosol parameter, it was decided to postpone the operational assimilation of profile data until further developments could be implemented in research mode.

Since the first effort. the development of the assimilation of aerosol backscatter profiles have gone a long way and more development is still envisaged. At the start of ACTRIS-2 project, the IFS was only able to assimilate the attenuated backscatter profile from CALIOP at one wavelength (532 nm). With ACTRIS-2, the code has been developed to be able to assimilate different types of instruments such as CALIOP, the EARLINET lidars, the ceilometers from E-PROFILE, and the Doppler wind lidar ALADIN onboard of Aeolus. Different wavelengths (355, 532 and 1064nm) can now be assimilated as well as different parameters (attenuated backscatter profile, backscatter profile, extinction profile) and from different viewing geometries (ground based or satellite). The developments have been such that now all profile information can be assimilated at the same time in the 4D-Var system.

In ACTRIS-2, the main experiments have been focusing on the assimilation of EARLINET data during the 72h campaign which had took place in July 2012 (Sicard 2012, D'Amico 2015). Operationally assimilated data have to be coded in Binary Universal Form for the Representation of meteorological data (BUFR) format. This format is not yet available for aerosol lidar backscatter. To be able to assimilate the data, a python code has been developed to convert the data to the ODB (Observation Data Base) format. This format is used only internally in IFS. However, it allows the direct injection of new observations in the assimilation process. This is permitted for research developments, but BUFR formation is still needed for a formal transition to operational implementation.

Figure 20 shows average profiles over Europe of aerosol backscatter before and after assimilation. It can be seen that the assimilation decreases the bias and the standard deviation of the analysis when compared to

the first guess indicating a successful assimilation. However, when plotting the data, it was noted that for three sites the longitudinal position of the lidar was wrongly assigned for 3 sites (Madrid, Evora and Granada), as shown in Figure 21. The bug is present in the original netcdf files where the longitude has been assigned as positive even for sites west of Greenwich. The data have been updated and the experiments re-run. The reason for the results still being possible was that the position of the instruments was not correct but neither completely unrealistic and the model was still trying to draw information from the observations. However, the direct plotting of the data allowed to reveal the problem. Feedback has been provided to the data providers.
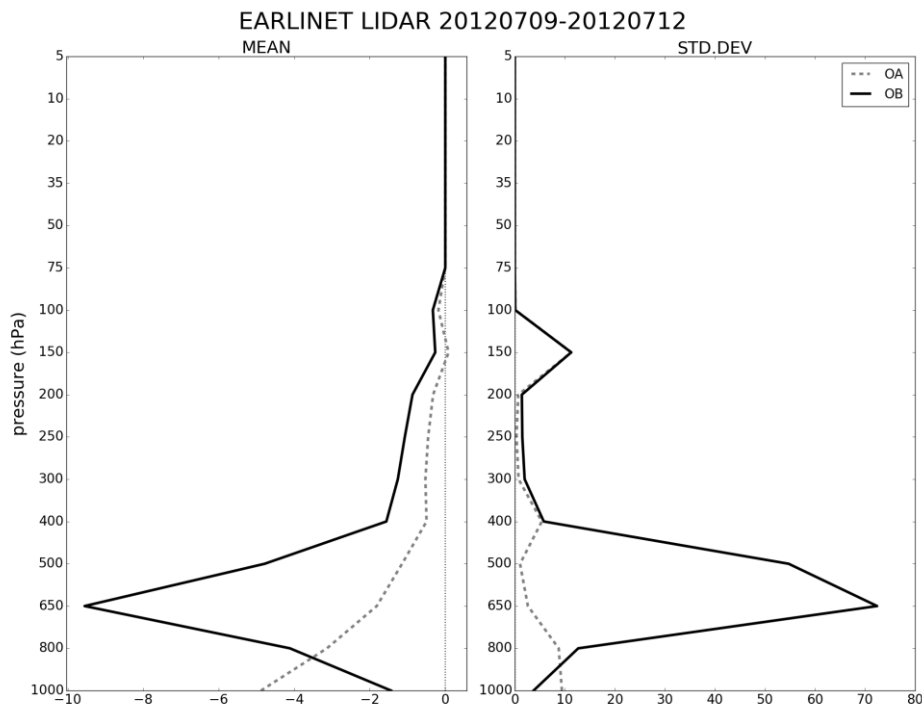

Figure 20. EARLINET observations minus analysis (dash), observations minus first guess (solid) standard deviation (right) and bias (left) for Europe. The data are assimilated for 3 days (09-12 July 2012), units of the horizontal axis are 10-7 (sr.m)$^{-1}$.
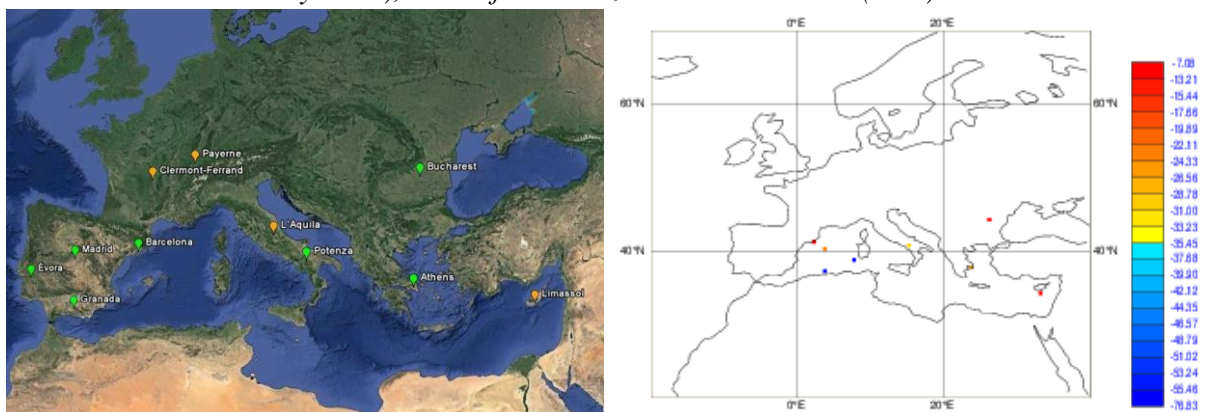

Figure 21. On the left, actual geographical position of the 11 stations EARLINET, green labels indicate advanced lidar systems; orange labels indicate Raman lidar systems, yellow circles indicate co-located sun photometers (Sicard 2015). On the right, observation minus first guess differences as seen by the 4D-Var. Note the wrong location of three stations.

In figure 22, a comparison between the AOD from AERONET (blue dot) and the AOD output of the model is presented. Two experiments are considered: one in which only the AOD from MODIS is assimilated (red) and one which uses MODIS AOD and the EARLINET LIDAR (green). The comparison is shown over one site equipped with a photometer and a lidar (Bucharest). The figure shows that the assimilation of the profile gives less weight to the AOD and that over all the assimilation of MODIS only is still performing better when compared with the AERONET observation. However, the fit of the assimilation AOD to the AERONET AOD is not perfect and the performance of the assimilation can still be improved. Indeed, for the 12th of July, the fit to the AERONET observations is better for the experiment which includes lidar data.
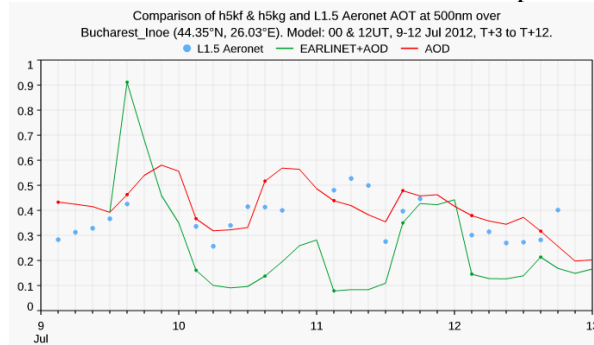

Figure 22. Comparison with AERONET of model AOD when only MODIS AOD is assimilated (red) and when the assimilation of MODIS AOD is coupled with the LIDAR from EARLINET (green) for Bucharest.

3.3.2 Investigation of the model bias

The assimilation of the LIDAR data from the special campaign in July 2012 does not give perfect results but is promising. Using the developments from ACTRIS-2, further studies have been performed. In the frame of the EUNADICS-AV project as well as via a collaboration with MeteoSwiss and E-PROFILE, different assimilation experiments have been performed. The following figures show the AERONET verification for three different assimilation experiments: Figure is relative to the 72h EARLINET assimilation, figure 24 is relative to an assimilation of the European ceilometers during the month of July 2018 including MODIS AOD (green) compared to MODIS only (red) and figure 25 is relative to the assimilation for the case of the Eyjafjallajökull eruption in 2010 of MODIS only (green), MODIS and CALIOP (red), MODIS and EARLINET (grey) and MODIS + prescribed volcanic emissions (orange). In the three cases, the impact on the bias of the model AOD with respect to the AERONET observations can be seen. The analysis of the Eyjafjallajökull case shows how each instrument is impacting the bias in a different way and hence the necessity to estimate the bias of each sets of instruments/observations. This will be pursued further using the variational Bias Correction (varBC) approach described in D13.3. At the time of writing, the varBC code related to lidar is not working properly and needs further debugging/development. The infrastructure is however ready for a full exploitation of ground-based lidar systems in conjunction with spaceborne lidars.
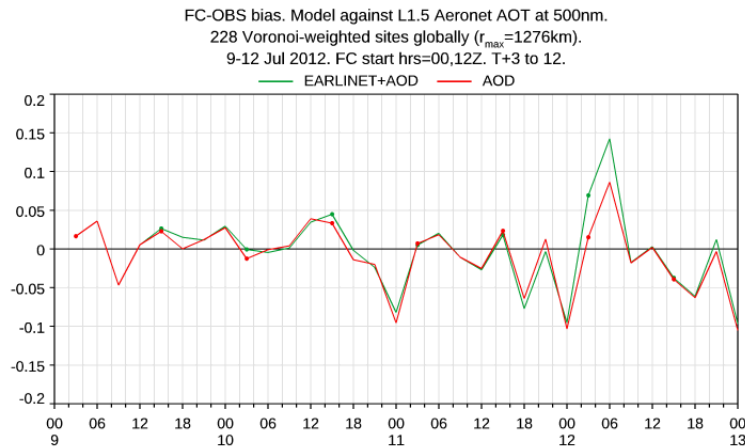
Figure 23. Evaluation of the global bias on the AOD from the model based on AERONET observations during the 72h EARLINET campaign 9-12 July 2012. In green, the experiment assimilating EARLINET lidar and MODIS AOD, in red the experiment assimilating only MODIS AOD. The impact of the EARLINET lidar is small but not negligible.
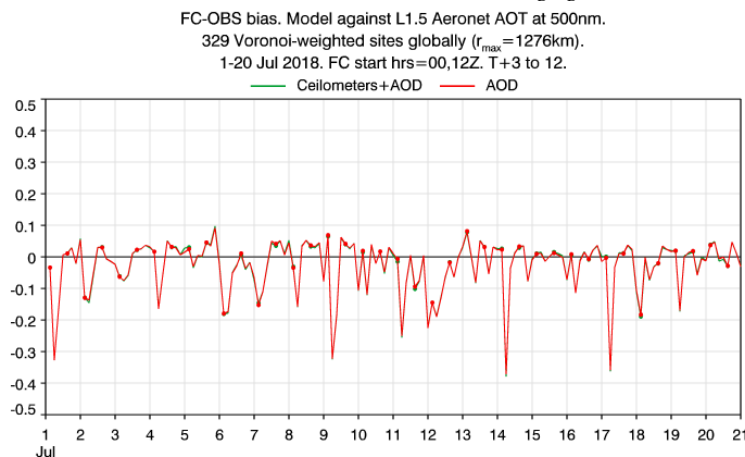
Figure 24. As for Figure but using the assimilation of ceilometer in conjunction with MODIS (green) and MODIS only (red) from period 1-21 July 2018. The global impact of the ceilometers is very small.
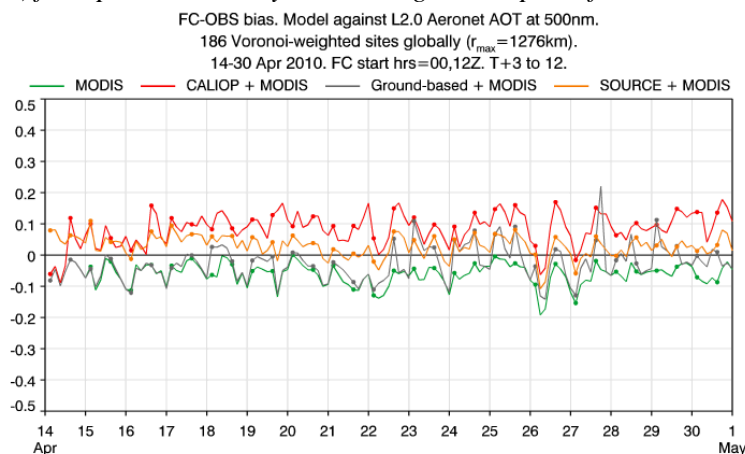
Figure 25. As for Figure during the Eyjafjallajökull eruption (14th April to 1st May 2010) using the assimilation of MODIS only (green), MODIS + CALIOP (red), MODIS + EARLINET LIDAR (grey) and MODIS + prescribed volcanic emission (orange).

ACTRIS (www.actris.eu) is supported by the European Commission under the Horizon 2020 – Research and Innovation Framework Programme, H2020-INFRAIA-2014-2015, Grant Agreement number: 654109

Page **26** / **30**

4 SUMMARY AND CONCLUSIONS

The objectives of the Joint Research Activity for model evaluation and assimilation activities were achieved. The results show of an impressive range of applications of ACTIS data. Both model evaluation and assimilation work has focused on different aspects, depending on the specific focus of the participating partner. For example, evaluation of dust extinction profiles has been explored for operational applications in the WMO Sand and Dust Storm Warning, Advisory and Assessment System which is jointly manages by the Barcelona Supercomputing Center and the Spanish Meteorological Agency (AEMET). Available NRT data from lidar and ceilometers were used to assess the BSC model skill in describing the vertical distribution of the dust. The extinction profile and the Center of Mass (CoM) were considered for the verification. Overall the agreement is encouraging, even if some model weaknesses were identified. In particular, the CoM seasonal variability is well represented in the model although an overall overestimation in the model is apparent. More systematic comparisons will allow to identify model improvements that can enable a better agreement with the observed profiles.

In support of the Copernicus Atmosphere Monitoring Service (CAMS) activities at ECMWF, a prototype of operational verification of aerosol light scattering has been implemented in JRA3. An ftp acquisition has been set-up between NILU and ECMWF. Data coming in NRT to the ACTRIS Data Centre are routinely acquired by ECMWF. The model provides scattering and absorption coefficients at all vertical levels and for different values of relative humidity. For the comparison with the measurements the surface values have been extracted in dry conditions (0% RH) and 50%RH. Measurements are usually referred to 40% RH, which means that the 0-50% range of model values should cover the observed range. Comparisons have been performed over one year from November 2016 to November 2017. Results show a good agreement for sites which are at low altitude and on relatively flat terrains. For mountain sites the comparison is not good due to the fact that the model values are relative to an altitude which might not be the one of the measuring stations. This is an effect of the coarse horizontal resolution of the model (80km). For mountain sites a special treatment involving the use of higher resolution topography to select the correct model level, needs to be applied in order to compare model and observation in a fair manner. This research development will become operational as part of the in-house verification activities of CAMS.

As far as assimilation activities were concerned, diverse applications were also pursued. For example, RIUUK demonstrated the use of lidar profiles for the improvement of the model description of the Eyjafjallajökull eruption, particularly relative to the plume height. An ensemble approach was taken to describe model uncertainties and extract more information from the observations. Results show that the analysis provided a better description of the plume characteristics. A similar successful assimilation but applied to dust extinction profiles was achieved at BSC where an Ensemble Kalman filter was used to provide analysis of dust profiles constrained with lidar data from the Dakar instrument operated by University of Lille. The impact of the observations was not only restricted to the analysis time but persisted several hours into the forecast demonstrating the positive impact that profile data can have on the forecast of aerosol fields. Other case studies were also investigated, with similar good impact of the data. At ECMWF ACTRIS lidar profiles from the Intensive Observing Campaign of 2012 were successfully assimilated in the operational 4D-Var system which is used in CAMS. Model lidar profiles in the analysis had a lower bias and standard deviation than background profiles with respect to the assimilated observations indicating a successful technical test. The systems capability were expanded to include both ground-based systems, including ceilometers, and spaceborne sensors with the goal to monitor and ultimately estimating the bias of spaceborne lidars with the high-accuracy ground-based systems. This goal has been partially achieved with the possibility to simultaneously monitor and assimilate CALIOP and ALADIN data alongside EARLINET/ACTRIS profiles. Further developments are necessary in order to estimate biases using the variational bias correction approach, operationally used for the assimilation of Aerosol Optical Depth (AOD) in CAMS.

Overall the activity was extremely successful thanks also to the direct collaboration of the model developers with the Data Centres and the data providers. Model analysis which are constrained by the ACTRIS observations can be considered very sophisticated level 3 products in their own right since they provide inside on aspects that cannot be directly given by the ACTRIS observations (i.e. underlying meteorology or

ACTRIS (www.actris.eu) is supported by the European Commission under the Horizon 2020 – Research and Innovation Framework Programme, H2020-INFRAIA-2014-2015, Grant Agreement number: 654109

Page **27** / 30

dust /volcanic aerosol emissions). It is hope that this collaboration can be continued. New avenues are being sought, through funding from Copernicus, H2020 as well as the European Space agencies (ESA and EUMETSAT). The legacy of the JRA3 in ACTRIS-2 will surely continue beyond the end of the project.

5 REFERENCES

Ansmann, A., Tesche, M., Seifert, P., Groß, S., Freudenthaler, V., Apituley, A., Wilson, K. M., Serikov, I., Linné, H., Heinold, B., Hiebsch, A., Schnell, F., Schmidt, J., Mattis, I., Wandinger, U., and Wiegner, M.: Ash and fine-mode particle mass profiles from EARLINET-AERONET observations over central Europe after the eruptions of the Eyjafjallajökull volcano in 2010, J. Geophys. Res., 116, D00U02, doi:10.1029/2010JD015567, 2011.

Ansmann, A., P. Seifert, M. Tesche and U. Wandinger, Profiling of fine and coarse particle mass: case studies of Saharan dust and Eyjafjallajökull/Grimsvötn volcanic plumes, Atmos. Chem. Phys., 12, (20), 9399–9415, 2012.

Benedetti, A. J.-J. Morcrette, O. Boucher, A. Dethof, R. J. Engelen, M. Fisher, H. Flentje, N. Huneeus, L. Jones, J. W. Kaiser, S. Kinne, A. Mangold, M. Razinger, A. J. Simmons and M. Suttie: Aerosol analysis and forecast in the European Centre for Medium‐Range Weather Forecasts Integrated Forecast System: 2. Data assimilation, JGR, https://doi.org/10.1029/2008JD011115, 2009.

Benedetti A. and A. Dabas: Assessment of the necessary developments to assimilate Aeolus and EarthCARE aerosol profile products, ESA Technical Note. Project AO/1-8242. Available upon request from ECMWF, 2016.

Binietoglou, I., S. Basart, L. Alados-Arboledas, V. Amiridis, ...U. Wandinger, and J. Wagner: A methodology for investigating dust model performance using synergistic EARLINET/AERONET dust concentration retrievals, Atmos. Meas. Tech., 8, 3577-3600, doi:10.5194/amt-8-3577-2015, 2015.

Bovchaliuk, V., Goloub, P., Podvin, T., Veselovskii, I., Tanre, D., Chaikovsky, A., Dubovik, O., Mortier, A., Lopatin, A., Korenskiy, M., and Victori, S.: Comparison of aerosol properties retrieved using GARRLiC, LIRIC, and Raman algorithms applied to multi-wavelength lidar and sun/ skyphotometer data, Atmos. Meas. Tech., 9, 3391-3405, doi:10.5194/amt-9-3391-2016, 2016.

D'Almeida, D. A.: On the variability of desert aerosol radiative characteristics, J. Geophys. Res., 92, 3017–3026, doi:10.1029/JD092iD03p03017, 1987.

D'Amico, G., Amodeo, A., Baars, H., Binietoglou, I., Freudenthaler, V., Mattis, I., Wandinger, U., and Pappalardo, G.: EARLINET Single Calculus Chain – overview on methodology and strategy, Atmos. Meas. Tech., 8, 4891-4916, https://doi.org/10.5194/amt-8-4891-2015, 2015.

Di Tomaso, E., Schutgens, N. A. J., Jorba, O., and Pérez García-Pando, C.: Assimilation of MODIS Dark Target and Deep Blue observations in the dust aerosol component of NMMB-MONARCH version 1.0, Geosci. Model Dev., 10, 1107-1129, doi:10.5194/gmd-10-1107-2017, 2017.

Gasteiger, J., S. Gross, V. Freudenthaler and M. Wiegner, Volcanic ash from Iceland over Munich: mass concentration retrieved from ground-based remote sensing measurements, Atmos. Chem. Phys., 11, (5), 2209–2223, 2011.

Ginoux, P., Chin, M., Tegen, I., Prospero J. M., Holben, B., Dubovik, O., Lin, S.-J.: Sources and distributions of dust aerosols simulated with the GOCART model, Journal of Geophysical Research, 106, D17, 20,255-20,273, 2001

Grimit, E. P. and C. F. Mass, Measuring the ensemble spread-error relationship with a probabilistic approach: Stochastic ensemble results, Month. Weath. Rev., 135, (1), 203–221, 2007.

Hess, M., P. Koepke, and I. Schult: Optical Properties of Aerosols and Clouds: The software

package OPAC, Bull. Am. Met. Soc., 79, 831-844, 1998.

Hollingsworth A. et al: Toward a monitoring and forecasting system for atmospheric composition: The GEMS Project, BAMS, https://doi.org/10.1175/2008BAMS2355.1, 2008.

Holben B., et al,: An emerging ground‑based aerosol climatology: Aerosol optical depth from AERONET, JGR, https://doi.org/10.1029/2001JD900014, 2001.

Hunt, B. R., Kostelich, E. J., and Szunyogh, I.: Efficient data assimilation for spatiotemporal chaos: A local ensemble transform Kalman filter, Physica D, 230, 112–126, 2007.

Janjic, Z. I. and Gall, R.: Scientific documentation of the NCEP nonhydrostatic multiscale model on the B grid (NMMB) – Part 1 Dynamics, Technical Report, NCAR/TN-489+STR, 2012.

Kaufman, Y. J ., D. Tanré, O. Dubovik, A. Karnieli, and L. A. Remer: Absorption of sunlight by dust as inferred from satellite and ground-based remote sensing, Geophys. Res. Lett., 28, 1479–1482, 2001.

Lange, A. C., Observability of sudden aerosol injections by ensemble-based four-dimensional assimilation of remote sensing data, University of Cologne, Dissertation, 2018.

Marticorena, B. and Bergametti, G.: Modeling the atmospheric dust cycle: 1. design of a soilderived dust emission scheme, J. Geophys. Res., 100, 16415–16430, doi:10.1029/95JD00690, 1995.

Marticorena, B., Bergametti, G., Aumont, B., Callot, Y., N'Doumé, C., and Legrand, M.: Modeling the atmospheric dust cycle: 2. simulation of Saharan dust sources, J. Geophys. Res., 102, 4387–4404, doi:10.1029/96JD02964, 1997.

Mattis, I., D'Amico, G., Baars, H., Amodeo, A., Madonna, F., and Iarlori, M.: EARLINET Single Calculus Chain – technical – Part 2: Calculation of optical products, Atmos. Meas. Tech., 9, 3009-3029, https://doi.org/10.5194/amt-9-3009-2016, 2016.

Mishchenko, M. I., L. D. Travis, and A. A. Lacis: Scattering, Absorption, and Emission of Light by Small Particles. Cambridge University Press, Cambridge, 2002.

Papagiannopoulos, N., Mona, L., Amodeo, A., D'Amico, G., Gumà Claramunt, P., Pappalardo, G., Alados-Arboledas, L., Guerrero-Rascado, J. L., Amiridis, V., Kokkalis, P., Apituley, A., Baars, H., Schwarz, A., Wandinger, U., Binietoglou, I., Nicolae, D., Bortoli, D., Comerón, A., Rodríguez-Gómez, A., Sicard, M., Papayannis, A., and Wiegner, M.: An automatic observation-based aerosol typing method for EARLINET, Atmos. Chem. Phys., 18, 15879-15901, https://doi.org/10.5194/acp-18-15879-2018, 2018.

Pérez, C., Haustein, K., Janjic, Z., Jorba, O., Huneeus, N., Baldasano, J. M., Black, T., Basart, S., Nickovic, S., Miller, R. L., Perlwitz, J. P., Schulz, M., and Thomson, M.: Atmospheric dust modeling from meso to global scales with the online NMMB/BSC-Dust model – Part 1: Model description, annual simulations and evaluation, Atmos. Chem. Phys., 11, 13001–13027, doi:10.5194/acp-11-13001-2011, 2011.

Peuch, V-H and R.J. Engelen:Towards and operational GMES Atmosphere Monitoring Service ECMWF Newsletter, 2012.

Schutgens, N. A. J., Miyoshi, T., Takemura, T., and Nakajima, T.: Sensitivity tests for an ensemble Kalman filter for aerosol assimilation, Atmos. Chem. Phys., 10, 6583–6600, doi:10.5194/acp-10-6583-2010, 2010.

Sicard, M., D'Amico, G., Comerón, A., Mona, L., Alados-Arboledas, L., Amodeo, A., Baars, H., Baldasano, J. M., Belegante, L., Binietoglou, I., Bravo-Aranda, J. A., Fernández, A. J., Fréville, P., García-Vizcaíno, D., Giunta, A., Granados-Muñoz, M. J., Guerrero-Rascado, J. L., Hadjimitsis, D., Haefele, A., Hervo, M., Iarlori, M., Kokkalis, P., Lange, D., Mamouri, R. E., Mattis, I., Molero, F., Montoux, N., Muñoz, A., Muñoz Porcar, C., Navas-Guzmán, F., Nicolae, D., Nisantzi, A., Papagiannopoulos, N., Papayannis, A., Pereira, S., Preißler, J., Pujadas, M., Rizi, V.,Rocadenbosch,

F., Sellegri, K., Simeonov, V., Tsaknakis, G., Wagner, F., and Pappalardo, G.: EARLINET: potential operationality of a research network, Atmos. Meas. Tech., 8, 4587-4613, https://doi.org/10.5194/amt-8-4587-2015, 2015.

Terradellas, E., Nickovic, S., and Zhang, X.: Airborne dust: a hazard to human health, environment and society, WMO Bulletin, 64, 42–46, 2015.

Veselovskii, I., Goloub, P., Podvin, T., Bovchaliuk, V., Derimian, Y., Augustin, P., Fourmentin, M., Tanre, D., Korenskiy, M., Whiteman, D. N., Diallo, A., Ndiaye, T., Kolgotin, A., and Dubovik, O.: Retrieval of optical and physical properties of African dust from multiwavelength Raman lidar measurements during the SHADOW campaign in Senegal, Atmos. Chem. Phys., 16, 7013-7028, doi:10.5194/acp-16-7013-2016, 2016.

White, B. R.: Soil transport by winds on Mars, J. Geophys. Res., 84, 4643–4651, doi:10.1029/JB084iB09p04643, 1979.

Wiscombe, W. J., Improved Mie scattering algorithms, Appl. Opt., 19, (9), 1505–1509, 1980.

Zehner, C., Monitoring volcanic ash from space, in Proceedings of the ESA-EUMET-SAT workshop on the 14 April to 23 May 2010 eruption at the Eyjafjöll volcano, South Iceland. Frascati, Italy, 26–27 May 2010, 2010.

ACTRIS (www.actris.eu) is supported by the European Commission under the Horizon 2020 – Research and Innovation Framework Programme, H2020-INFRAIA-2014-2015, Grant Agreement number: 654109

Page **30 / 30**